SUBSTRATE SPECIFICITY OF METAL-DEPENDENT LYSINE DEACETYLASES

by

Caleb G. Joseph

A dissertation submitted in partial fulfillment
of the requirements for the degree of
Doctor of Philosophy
(Medicinal Chemistry)
in the University of Michigan
2012

Doctoral Committee:

Professor Carol A. Fierke, Chair
Professor Anna Mapp
Professor Ronald Woodard
Professor George Garcia

DEDICATION

I dedicate this thesis to my wonderful family for their unconditional love and support.

My late mother Louisiane, my father Georges, my step-mom Bernadette, my siblings: Alexandra, Junior, Athalie, Adrien, my in-law brothers Eric and Taylor, my nephew Taylen and my soon-to-arrive niece and nephew.

ACKNOWLEDGEMENTS

I owe my deepest gratitude to my advisor Dr. Carol Fierke for all her encouragement, guidance, support, and patience. I appreciate the infrastructure and resources that Carol provided for my studies.

I would also like to thank my committee, Drs. Anna Mapp, Ronald Woodard and George Garcia for their insightful comments and assistance.

Additionally, this work would not have been possible without my collaborators. Dr. Milan Mrksich and Dr. Micheal Scholle from the University of Chicago contributed to the mass spectrometry studies. Dr. Matthew Fuchtner, Imperial College London, did all the computational studies.

I would also like to thank my labmates. Namely, I am indebted to Sam Gattis and Stephanie Gannt for mentoring me on the deacetylase project. Andrea Stoddard for all her help raging from molecular cloning to conference reimbursement.

Last, I would like to thank the Medicinal Chemistry department for accepting me and supporting me through the years. Thanks to the department secretaries Regina Belainy and Sarah Lloyd for their kindness and guidance. Also, thanks to the students in the department for their help with classes, MC740, and prelim.

TABLE OF CONTENTS

LIST OF FIGURES

LIST OF SCHEMES

LIST OF TABLES

LIST OF ABBREVIATIONS

AcCoA	Acetyl - Coenzyme A
AP	Alkaline phosphatase
APC	Antigen presenting cells
AUC	Area under the curve
CD	Circular Dichroism
CREB	cAMP responsive element binding protein 1
FDL	Fluor-de-Lys assay
GABC	General acid/general base catalysis
H1	Histone H1
H2	Histone H2
H3	Histone H3
H4	Hisone H4
HDLP	Histone deacetylase like protein
HIV-TAT	human immunodeficiency virus (HIV-1) (transactivator of transcription
HSP90	Heat schock protein 90
ICP-MS	Inductively coupled plasma mass spectrometry
IL-10	Iterkeukin 10
IL-12	interleukin 12
IMAC	immobilized metal affinity chromatography (IMAC)
IPTG	Isopropyl β-D-1-thiogalactopyranoside
KAT	Lysine acetyl transferases
KDACi	Lysine deacetylase inhibitor
KDACs	Lysine deacetylases
LpxC	UDP-3-O-(R-3-hydroxymyristoyl)-GlcNAc deacetylase
MALI-TOF-MS	Matrix-assisted laser desorption-ionization time-of-flight mass spectrometry
MCA	4-methlyl-coumaryl-7-amide
MCM	mini-chromosome maintenance
MCS	Multiple cloning site
MD	Molecular dynamics
MDM2	Murine double minute
MOPS	3-(N-morpholino)propanesulfonic acid
MVC	Monovalent cations
NAD+	Nicotinamide Adenine Dinucleotide
NADH	Nicotinamide adenine dinucleotide hydride

QM/MM	Quantum mechanical / molecular mechanics
SAHA	Suberoylanilide hydroxamic acid
SUMO	Small Ubiquitin-like Modifier
TCEP	Tris(2-carboxyethyl)phosphine
TEV	Tobacco Etch Virus
TSA	Trichostatin A

ABSTRACT

SUBSTRATE SPECIFICITY OF METAL-DEPENDENT LYSINE DEACETYLASES

by

Caleb G. Joseph

Chair: Carol A. Fierke

Lysine deacetylases (KDACs) catalyze the deacetylation of acetylated lysine residues on histones and other protein substrates. This modification plays a vital role in numerous cellular processes and inhibitors targeting KDAC are effective in a variety of diseases. Eleven members of the 18-member KDAC family require a divalent metal ion for activity. Previous studies have demonstrated that the reactivity of KDAC8 varies with the bound metal ion (Co^{2+}> Fe^{2+} > Zn^{2+}). Here I show that the bound metal ion also regulates the substrate specificity of KDAC8. Incubation of metal-substituted KDAC8 with an acetylated peptide library identified peptides that were deacetylated more rapidly by either Zn^{2+}- or Fe^{2+}-KDAC8 and peptide substrates that display similar reactivity with both enzymes. The steady-state kinetic parameters measured for peptides from each specificity profile showed that the k_{cat}/K_M values recapitulate the results observed in the library screen confirming the metal-dependent substrate selectivity. These studies suggest the possibility that KDAC8 activity and specificity are regulated *in vivo* by Zn/Fe metal switching.

Furthermore, the reactivity of KDAC11, with peptide libraries demonstrates that the activity and specificity of this isozyme are also dependent on the bound metal ion. Furthermore, these selectivity screens led to the identification of a peptide sequence motif (GPK(ac)LGC) that corresponds to a sequence near the N-terminus of Cdt1 (IIAPPKLACRTPS), a proposed *in vivo* substrate for KDAC11. The value of the k_{cat}/K_M for the Zn^{2+}-bound KDAC11 on this sequence is increased by 1333-fold over the commercially available coumarin substrate to a value of 0.33 ± 0.04 $\mu M^{-1}s^{-1}$ and the reactivity with Fe^{2+}-KDAC11 is even higher (>0.5 $\mu M^{-1}S^{-1}$).

Finally I show that Arg37, a residue proposed to regulate the dissociation of acetate in KDAC8, is critical for the catalytic activity of KDAC8. Substitution of Arg37 with either alanine (R37A) or glutamate (R37E) decreases the value of k_{cat}/K_M by 528-fold and 4 x 10^5-fold, respectively. Furthermore, the R37A mutation decreases the affinity of KDAC8 for acetate by at least 3 kcal/mol, only slightly less than the energetic destabilization of the transition state (3.5 kcal/mol). The circular dichroism spectrum show that the secondary structure of KDAC8 is not affected by the R37A mutation but is altered by the R37E mutation. These results show that Arg37 is important for catalysis and acetate affinity, and could be exploited for preparing specific inhibitors of KDAC8.

CHAPTER I

INTRODUCTION

LYSINE DEACETYLASES BACKGROUND

Post-translational Protein Modification

Post-translational modifications are enzyme-catalyzed chemical modifications that increase the functional capabilities of many proteins in eukaryotic cells. Nascent or folded polypeptides are subject to numerous modifications including phosphorylation, prenylation, methylation, glycosylation, farnesylation, and acetylation. These modifications of protein sequence produce extraordinarily diverse functions in the proteome. Therefore it is not surprising that they are major regulatory mechanisms in many cellular processes like signaling, cellular localization, and protein association. Post-translational modifications can be irreversible or reversible. Reversible modifications frequently involve the addition and removal of a specific group by two functionally opposite enzyme reactions(1,2).

Protein Acetylation

One type of post-translational modification involves the acetylation of lysine residues. Protein lysine deacetylases (KDACs) catalyze the hydrolysis of acetylated lysine residues on proteins. Protein lysine acetyl-transferases (KATs) catalyze the reaction of acetyl-CoA with lysines residues to form acetyl-lysine (Scheme 1.1)(3,4). KDACs were originally termed HDACs (Histone Deacetylases) because lysine acetylation was first discovered on the N-termini of histone proteins. Since DNA wraps around histone proteins (H2A, H2B, H3, H4) to form the chromatin structure, the dynamics of KATs and KDACs can dramatically alter interactions between the transcriptional machinery and the DNA, essentially linking these post-translational modifying enzymes to gene transcription(5,6). Generally, acetylation of lysines on histone proteins leads to a loosening of the chromatin structure, providing transcriptional activators greater access to the DNA and facilitating transcription. Overexpression of KDACs markedly decreases the global acetylation of the histone proteins, thereby hindering the binding of transcriptional activators and suppressing the expression of appropriate genes. This pattern of gene expression is a hallmark of aberrant tumor cell division, growth and invasion(7). Expanded studies on the effect of KDACs on gene expression resulted in the identification more than 1000 eukaryotic proteins and non-protein molecules, like polyamine, that are acetylated. The acetylome, like the phosphoproteome, is now composed of more than 3000 protein substrates. However, a relatively small number of enzymes catalyze these post-translational modifications(8-11).

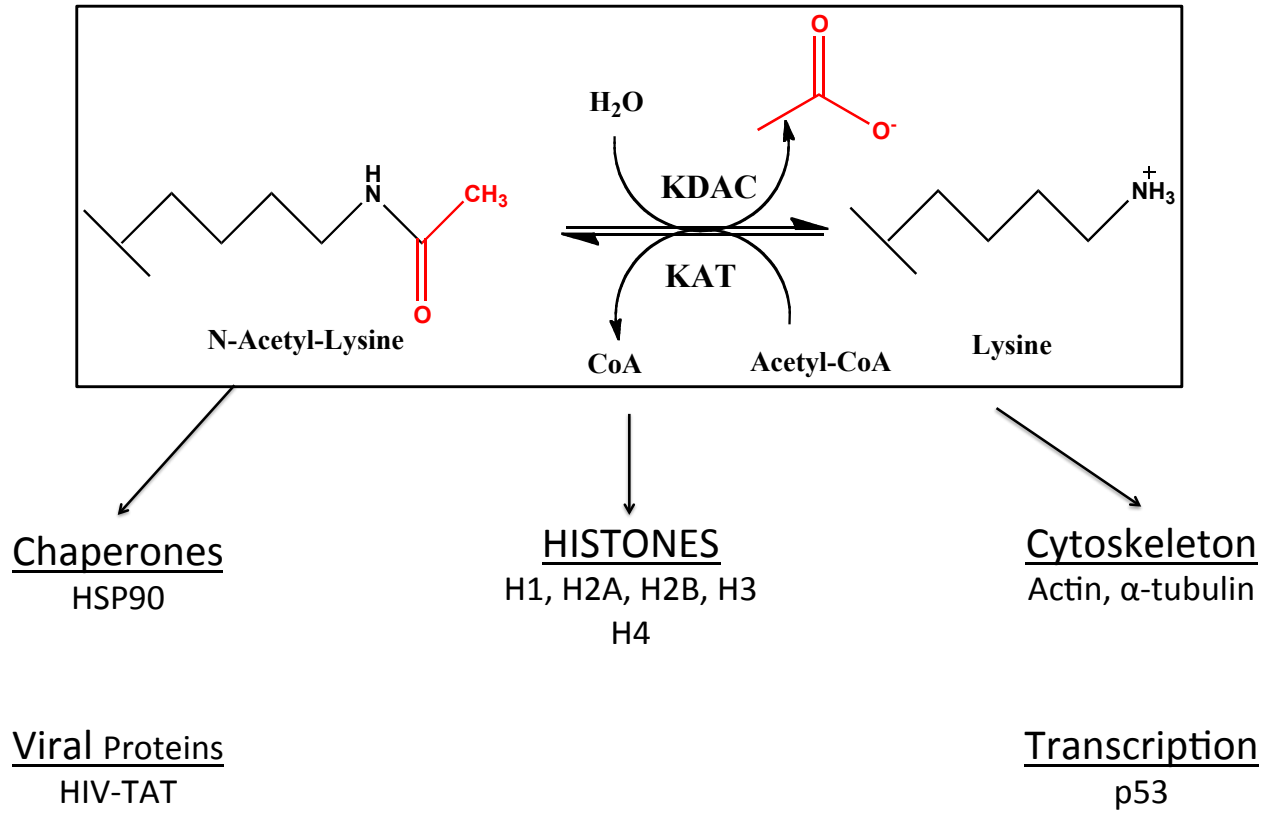

Scheme 1.1. KDACs and KATs Reactions in Diverse Cellular Processes. A protein modified by reversible acetylation represents each process.

The Human KDAC Superfamily

The eukaryotic genome encodes 18 KDACs that are divided into 4 classes based on sequence homology, cellular localization and function(12). The metal-dependent KDACs include Class I, II, and IV (Figure 1.1). Class I consists of KDAC (1-3, 8). Class I KDACs are ubiquitously expressed and reside primarily in the nucleus(13). KDAC1 and KDAC2 share high sequence homology and they interact with nucleosome remodeling complexes Sin3, NuRD, and Co-REST, while KDAC3 is part of the co-repressor complexes SMRT and N-CoR(14). KDAC8 is the only KDACI isozyme not commonly observed in large protein complexes(15,16). The deacetylase activities of KDAC isozymes 1-3 have only been observed in multi-protein complexes and these enzymes are inactive when expressed recombinantly(17). KDAC8 has been extensively characterized and is the model system for studying mammalian KDACs. KDAC isozymes 4,5,6,7,9, and 10 are class II enzymes(16). Class II is further subdivided into class IIa (KDAC4, 5, 7, 9) and Class IIb (KDAC 6, 10). Class IIa KDACs contain a distinct large N-terminal domain and expression pattern. KDAC4 is highly expressed in the brain and growth plates of the skeleton. KDAC5 and 9 are mostly found in the muscles and heart and KDAC7 is enriched in endothelial cells and thymocytes(18,19). Class IIb isozymes (KDAC6 and KDAC10) feature an extra deacetylase domain and shuttle frequently between the cytoplasm and the nucleus. KDAC6 is a cytoplasmic regulator of HSP90 that features two deacetylase domains and a zinc-finger domain(20,21). Class I and Class II KDACs require a divalent metal ion cofactor for activity. Also, these enzymes have homologous active sites except for a Tyr residue that

is conserved in Class I and substituted by a His in Class II(22). Class III enzymes (the Sirtuin family) has 11 members, utilize an NAD cofactor to catalyze deacetylation by a completely different mechanism and will not be covered here (23). KDAC11 is the lone member of class IV. KDAC11 is expressed in the brain, heart, muscles, testis and kidney tissues and proposed to be important in immune function(24).

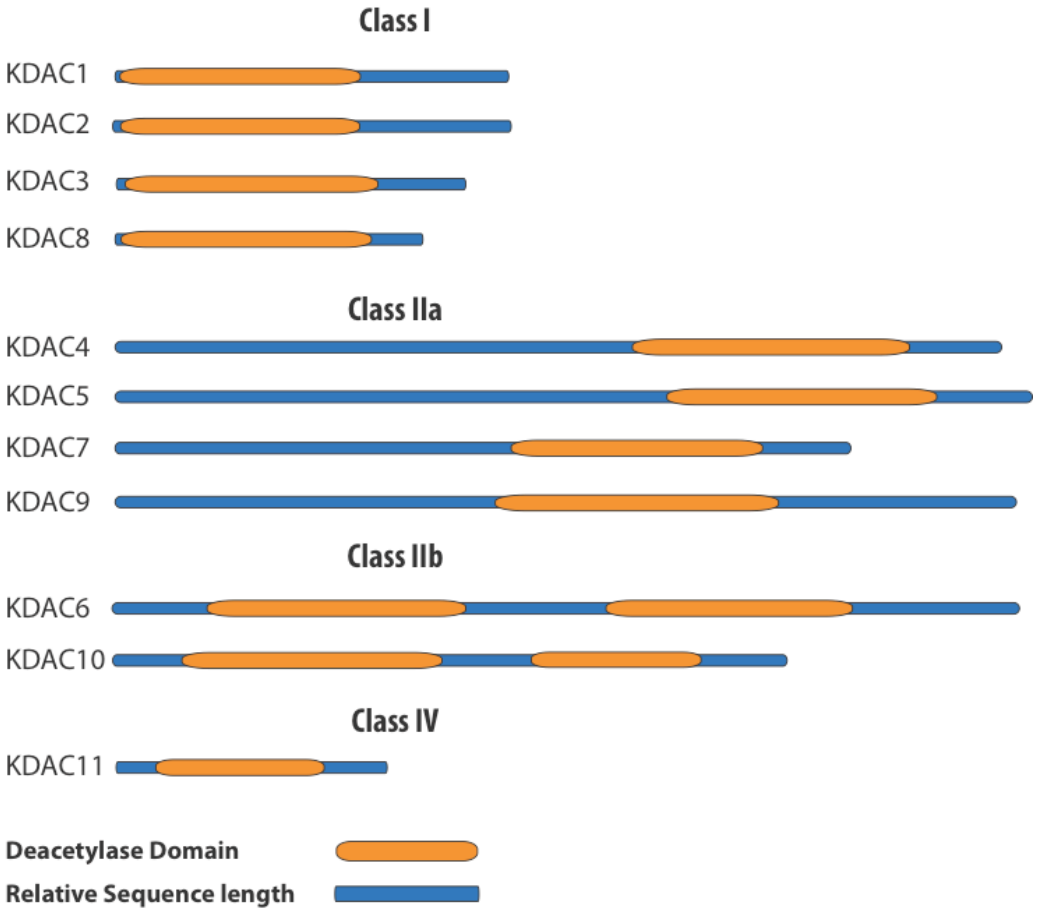

Figure 1.1. Classes of Human Metal-dependent KDACs

Roles of KDACs in Eukaryotic Cells

KDAC enzymes play a fundamental role in modulating cellular processes. The balance between KDAC and KAT activities is critical for maintaining proper chromatin structure as well as the biological function of many proteins(25). Unregulated KDAC activities lead to both expression and suppression of genes, depending on the context. Sustained KDAC activity restricts the access of the transcriptional machinery to genes that are responsible for growth arrest, differentiation, and apoptosis. Vorinostat and Romedopsin (Table 1.1), two inhibitors that specifically target KDACs *in vitro*, have been approved by the FDA for the treatment of cutaneous T-cell lymphoma(26). Although the cellular mechanism of these inhibitors is still under investigation, *in vitro* data show that these are very potent inhibitors of KDACs, especially KDAC8 (50 nM), implicating KDAC inhibition as the *in vivo* mode of action(27). Furthermore, acetylation of histone H4 at Lys 16 (H4K16) and histone H2B at lysines 11 and 16 (H2BK11, K16) suppresses the DNA affinity of transcriptional co-activators indicating that deacetylation at these positions is important for transcriptional activity. Additionally, binding of the transcriptional activator Bromodomain 1 (Bdf1) to DNA is inhibited by the mutation of H4 K12R but not by the H4 K16R mutation(28-30). These results strongly suggest that a fine-tuned regulation of KDAC activity is vital for determining the correct chromatin configuration.

In addition to histone proteins, KDACs regulate the activity of more than 3000 proteins in eukaryotic cells(25). For instance, deacetylation of the oncogenic protein Survivin by KDAC6 leads to relocalization to the cytoplasm where it functions as an

anti-apoptotic factor(31). Therefore, unchecked KDAC6 activity maintains Survivin localization in the cytoplasm. Conversely, inhibition of KDAC6 leads to the accumulation of acetylated Survivin at Lys 129 catalyzed by the KAT CREB-binding protein, which promotes relocalization of Survivin to the nucleus. Secondly, KDAC8 is highly expressed in cells undergoing smooth muscle differentiation; specifically, KDAC8 associates with smooth muscle α-actin and facilitates smooth muscle contraction. RNAi knockdown of KDAC8 in smooth muscle cells hinders the contraction of collagen lattices(15,32). Finally, KDAC3 differentially regulates the activity of nuclear NF-kappaB by deacetylating two lysines on its subunit(33,34). Altogether, these observations illustrate the significance of proper regulation of KDAC activities in a variety of cellular processes.

Lysine acetylation of proteins in cells also protects them from degradation by the proteasome. E3 ubiquitin ligases catalyze the addition of ubiquitin (76 amino acid long peptide) to unprotected lysine residues for subsequent degradation by the proteasome(35). As a result, competition between the KATs and E3 ligases directly influences the stability of protein substrates in the cell(36). For example, deacetylation of the tumor suppressor P53 renders it a good substrate for the E3 ubiquitin ligase activity of MDM2. HDAC1 is commonly found in complex with MDM2 and has been shown catalyze the deacetylation of P53, which is then ubiquitinated and degraded(37,38). Similarly, Smad7, a member of the Smad complexes that participate in the Transforming Growth Factor ß (TGFß) signaling cascade, is acetylated at Lys64 and Lys70 catalyzed by the transcriptional co-activator P300. This acetylation competes with ubiquitination catalyzed by the Smurf 1 and Smurf 2 E3 ligases at these sites and

prevents the deleterious consequences of a faulty TGFß signaling cascade(39,40). Therefore, the balance between KAT and KDAC activities helps maintain a stable concentration of many proteins in mammalian cells.

Inhibition of KDACs

Interestingly, KDAC inhibitors (KDACi) were identified before KDAC enzymes. The administration to cells of Trapoxin, a cyclic tetra peptide, caused an increase in acetylation of histone proteins, leading to the hypothesis that the deacetylation of histones was inhibited(41,42). Three years later, Grunstein and colleagues isolated KDAC1 using a Trapoxin-labeled affinity tag. Sequence analysis later revealed that KDAC1 is highly homologous to yeast KDAC Rdp3(43,44). These discoveries led to the identification of the rest of the mammalian KDAC protein family. In recent years, KDACi have been a powerful experimental tool for investigating the functional role of KDACs. Now KDACi are structurally diverse compounds that are also classified according to their common structural scaffold (Table 1.1). These structures include hydroxamates, cyclic peptides, aliphatic acids, and benzamides(6). Suberoylanilide hydroxamic acid (SAHA), the first KDACi approved by the FDA, is a hydroxamic acid that inhibits class I and class II

A)

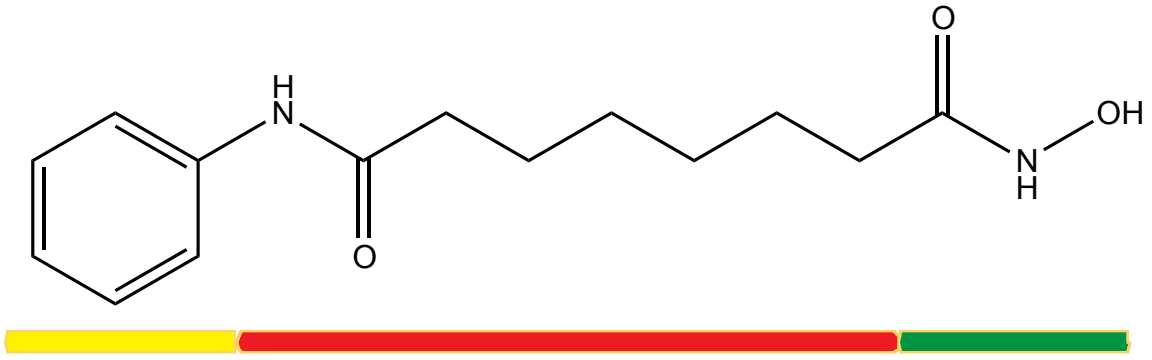

B)

Compound Class	Example	Structure	Target	Potency
Hydroxymates	SAHA	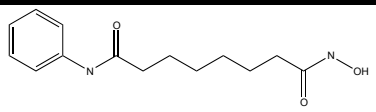	Class I, II, IV	nM
Cyclic peptides	FK-228	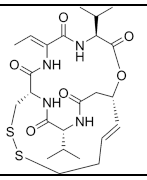	Class I	nM
Benzamide	MS-275	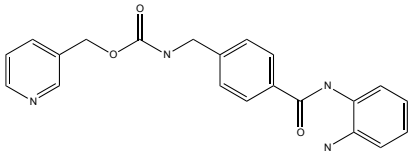	Class I	μM
Aliphatic Acid	Phenyl Butyrate	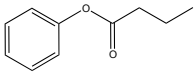	Class I, II	mM

Table 1.1. Structural Classes of KDACi. (A) KDACi pharmacophore model. (B) KDACi structures, class selectivity and potency.

KDACs. It consists of a capping group, a linker moiety similar to the lysine chain, and the hydroxymate, which chelates the active site metal ion. Romidepsin, the second FDA-approved KDACi, represents the cyclic peptide class. This molecule is a prodrug that requires reduction of the disulfide bond in the cell to gain effectiveness. Like the hydroxymate class, it contains a larger capping moiety. Reduction of the disulfide bond yields a linker mimicking lysine and a thiol side chain that coordinates the metal(45). The aliphatic acids inhibitors have a shorter linker and are generally weak KDAC inhibitors ($K_i \approx$ mM). The pharmacophores of the KDACi are the capping group, the linker and the metal binding moiety(46). The requirement for the metal binding moiety was identified when the first crystal structure of a KDAC was solved.

Structural Analysis of KDACs

The first structural representation of KDACs came from the crystal structure of the histone deacetylase homologue (HDLP) from *Aquifex aeolicus*(47). Structural characterization shows an α/β fold that features an 11 Å-deep pocket leading to the active site and a 14 Å internal channel protruding away from the active site. The structure also shows well-defined loops (L1-L7). In the Zn^{2+} complex HDLP structure, L3 and L7 contain conserved residues (Asp178, Asp267, His180) that coordinate the Zn^{2+} ion. The 11 Å deep pocket accommodates the substrate in an orientation that positions the acetylated lysine in the active site, near the catalytic metal ion. The internal channel is composed of mainly of hydrophobic residues, except for Arg 27 and His 21 that are proposed to facilitate acetate dissociation. Later, the crystal structure of KDAC8 bound to

the inhibitor trichostatin A (TSA) was solved and the enzyme retains many of the features observed in HDLP(48). It has an 8 stranded parallel ß-sheet flanked by 11 α-helices. In addition to the Zn^{2+} ion, there are two bound K^{+} ions, located 7 and 21 Å from the zinc binding site, respectively. These potassium ions stabilize KDAC8 since circular dichroism spectroscopy shows global unfolding of the enzyme in their absence. The Zn^{2+} ion is penta-coordinated by Asp178, Asp267, His180, a water molecule and the hydroxymate moiety of TSA (Figure 1.2). The inhibitor coordinates the zinc ion, in addition to conserved residues His 142 and His 143 and fits into the deep pocket. The entrance of the active site cleft is lined by loops, which suggests flexibility in the binding of diverse substrates, as necessary for the large acetylome.

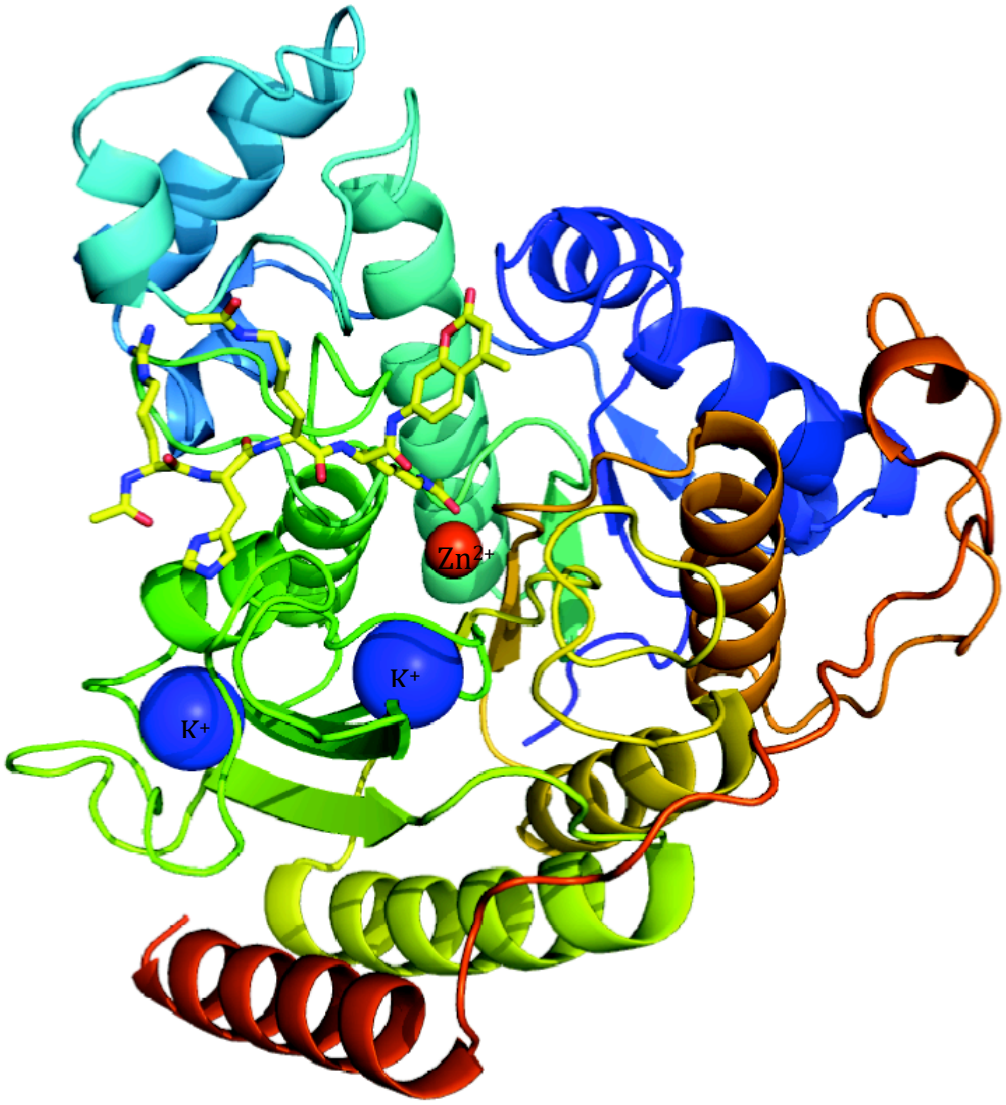

Figure 1.2. Crystal Structure of Human KDAC8 bound to TSA

Catalytic Mechanism of KDACs

The catalytic mechanism of KDACs proposed from the crystal structure of HDLP and KDAC8 mirrors the metal-dependent mechanism of UDP-3-O-(R-3-hydroxymyristoyl)-GlcNAc deacetylase (LpxC)(49,50). Mammalian KDACs, with the exception of Sirtuins, have homologous active sites, including the residues that chelate the bound divalent metal. Based on these observations, it is proposed that their catalytic mechanisms are also analogous (Scheme 1.2). The catalytic metal site is pentacoordinated by an Asp_2His triad, the substrate and a water molecule. This is an unusual ligand set for zinc enzymes. Key residues consist of two adjacent histidine residues (His142, His143) that are oriented by interaction with aspartate side chains (Asp 176, Asp183, respectively) that position the His groups during catalysis. His142 and His143 were proposed to act as a general acid/general base (GABC) pair and Tyr306 was proposed to stabilize the oxyanion transition state and intermediate (Scheme 1.2). Hydrolysis of the acetylated-lysine occurs when the catalytic metal ion and the His143 activate a water molecule for nucleophilic attack on the substrate's carbonyl to form an oxyanion tetrahedral intermediate that is stabilized by formation of a hydrogen bond with Tyr306. His142 is proposed to serve as the general acid to protonate the lysine amide during the breakdown of the tetrahedral intermediate to yield acetate and lysine(51,52). An alternative mechanism suggested from mutagenesis, pH profile and *Ab Initio* QM/MM MD studies is that His143 is a bifunctional GABC while His142 stabilizes the oxyanion intermediate (Scheme 1.2). The H143A mutation in KDAC8 causes a 94000-fold decrease in k_{cat}/K_m whereas the H142A mutation decreases activity by only 360-fold,

which diminishes the importance of His142 as a general acid catalyst. *Ab initio* QM/MM MD simulation of the reactant states of KDAC8 suggested that only the singly protonated His142 and His143 allow the formation of a pentacoordinated Zn^{2+} atom with proper ligand distances for catalyzing deacetylation. Furthermore, the free energy activation barrier calculated from this same simulation is 18.3 kcal/mol, comparable to the value calculated from k_{cat}(catalyzed)/k_{cat}(uncatalyzed)(53-55). Together these results point to a mechanism where His143 both functions as a general base that accepts a proton for the Zn^{2+}-bound water and acts as a general acid to protonate the leaving group. His142 is proposed to function as an electrostatic catalyst to stabilize the transition state.

Although the precise roles of His142 and His143 are still under investigation, the importance of Tyr306 for activating has been established. Tyr306 is substituted for a His in Class IIa KDACs and their deacetylase activity is significantly slower compared to class I KDACs(22,56). The substrate bound KDAC8 crystal structure was solved with Tyr306 mutated to Phe demonstrating that this residue is critical for turnover and less important for substrate binding. Furthermore, this Y306F mutation decreases activity by 145-fold. Substrate binding is mediated by Asp101, which is conserved across the KDAC family except KDAC11 (Figure 1.3). D101 makes two hydrogen bonds with the peptide substrate. The first is with the backbone NH group of the scissile lysine residue and the second contacts the backbone NH group of the adjacent residue (n+1). The D101A mutation disrupts these interactions and substantially decreases catalytic activity by 200-fold(22,55).

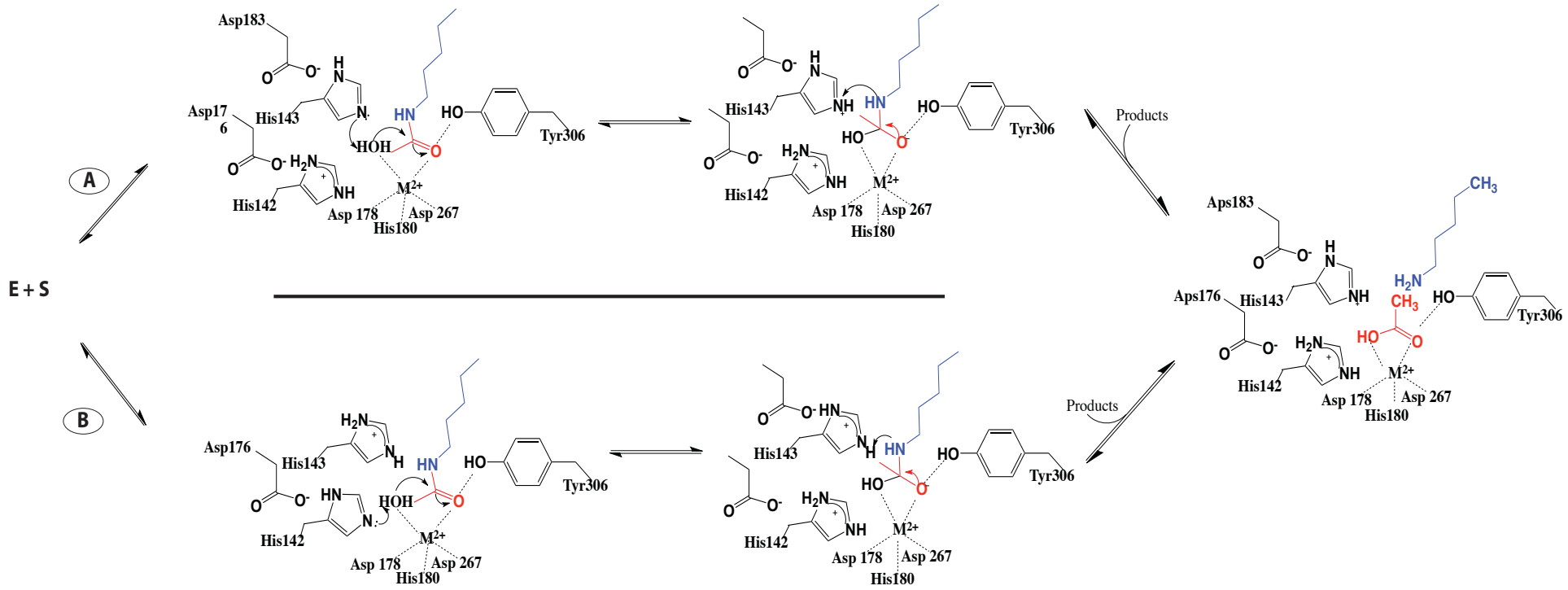

Scheme 1.2. Proposed KDAC Mechanisms. A) H143 acts as a bifunctional GABC and H142 as an electrostatic catalyst. B) GABC pair: His142 behaves like a GBC and His143 is the GAC.

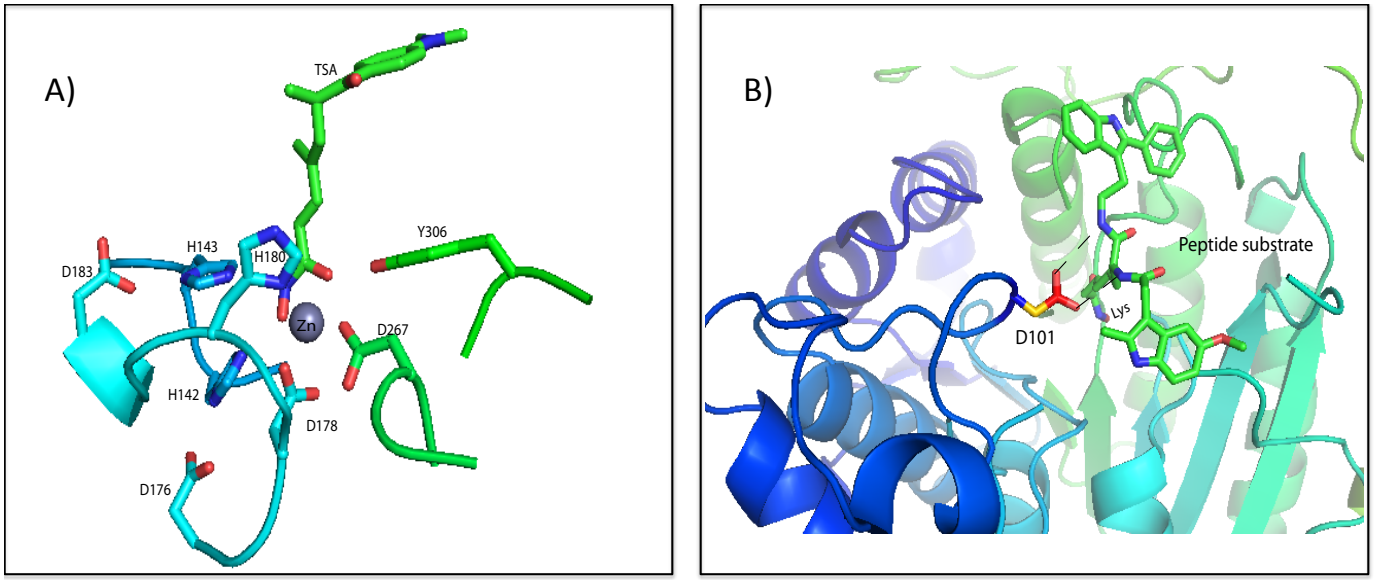

C)

Enzymes	*D101*	*H142*	*H143*			*D176*		*D178*		*D183*	*D267*		*H180*			*Y306*
KDAC1	**D**	**H**	**H**	A	Y	**D**	I	**D**	I	**D**	**D**	I	**H**	G	G	**Y**
KDAC2	**D**	**H**	**H**	A	Y	**D**	I	**D**	I	**D**	**D**	I	**H**	G	G	**Y**
KDAC3	**D**	**H**	**H**	A	Y	**D**	I	**D**	I	**D**	**D**	I	**H**	G	G	**Y**
KDAC8	**D**	**H**	**H**	A	Y	**D**	V	**D**	L	**D**	**D**	L	**H**	G	G	**Y**
KDAC4	**D**	**H**	**H**	A	I	**D**	V	**D**	W	**N**	**D**	V	**H**	G	G	**H**
KDAC5	**D**	**H**	**H**	A	I	**D**	V	**D**	W	**N**	**D**	I	**H**	G	G	**H**
KDAC6-N	**D**	**H**	**H**	A	I	**D**	V	**D**	W	**Q**	**D**	V	**H**	G	G	**Y**
KDAC6-C	**D**	**H**	**H**	A	L	**D**	V	**D**	W	**N**	**D**	V	**H**	G	G	**Y**
KDAC7	**D**	**H**	**H**	A	I	**D**	V	**D**	W	**N**	**D**	V	**H**	G	G	**H**
KDAC9	**D**	**H**	**H**	A	I	**D**	V	**D**	L	**N**	**D**	V	**H**	G	G	**H**
KDAC10	**D**	**H**	**H**	G	V	**D**	V	**D**	W	**Q**	**D**	V	**H**	G	G	**Y**
KDAC11	**N**	**H**	**H**	C	I	**D**	I	**D**	L	**N**	**D**	A	**H**	G	G	**Y**

Figure 1.3. Substrate binding site and sequence alignment of metal-dependent KDAC isozymes. A) View of the residues that line the active site and coordinate the bound metal ion. B) View of Asp101 interaction with the bound peptide substrate. C) Sequence alignment of metal-dependent KDAC isozymes showing the conversed catalytic residues.

Metal Ion Function

Divalent metal cations are essential catalytic and structural cofactors in many enzymes. Among the most abundant trace metals in eukaryotic cells are the transition row metals Zn^{2+}, Cu^{2+}, and Fe^{2+}[57,58]. Metal-dependent lysine deacetylases use a single catalytic metal cation. The catalytic metal ion accepts electrons from the nucleophile to lower the pK_a of this group, neutralizes the negative charge in the substrate to enable the approach of the nucleophile, and stabilizes the transition state. At the active site, protein side chains coordinate and modulate the metal ion. Removal of the catalytic metal by incubating with chelating agents like dipicolinic acid (DPA) and ethylenediamine tetra acetic acid (EDTA) inhibits deacetylase activity.

A compelling feature of the enzymes is their ability to retain high catalytic activity with a variety of bound metals including Ca^{2+}, Zn^{2+} and Fe^{2+}(59). These enzymes achieve this by capitalizing on the flexibility of the inner and outer-shell coordinating ligands to form a reactive complex, in addition to the intrinsic properties of the divalent metal cations. Indeed, transition row metals like Fe^{2+} and Zn^{2+} are strong Lewis acids. As a Lewis acid, the metal lowers the pK_a of coordinated ligands and enhances reactivity around neutral pH. The Lewis acidity trend for common cofactors for the metal-deacetylases is $Cu^{2+} > Ni^{2+} > Zn^{2+} > Co^{2+} > Fe^{2+}$. In addition to Lewis acidity, the coordination geometry, oxidation state, and ligand exchange kinetics are vital during the course of the hydrolysis reaction. The coordination preference for Zn^{2+} is tetrahedral (4 ligands), while Fe^{2+} and Co^{2+} prefer octahedral (6 ligands) and Cu^{2+} frequently adopts a linear geometry (2 ligands). Zn^{2+} is the only transition metal with a shell full of D-electrons and therefore is redox insensitive, whereas, Fe^{2+}, Cu^{2+}, Ni^{2+}, and Cu^{2+} are all

redox active(60-62). The redox insensitivity of Zn^{2+} can be beneficial to KDAC activity especially during periods of redox stress. The structural properties of the divalent metal ion can stabilize a specific conformation in the overall KDAC structure that enhances substrate selectivity. Given the large number of acetylated proteins in mammalian cells, metal-induced substrate recognition could be a vital aspect of KDAC mechanism.

Objectives of this work

Enormous progress has been made in advancing our understanding of enzymatic deacetylation in mammalian cells. So far, 18 KDACs have been identified and their characterization is rapidly expanding. These studies have revealed the diverse role of these KDACs in the regulation of gene expression as well as the biological function of many proteins in the cell. Expression studies in human tissues show that most KDACs are expressed ubiquitously, except for Class II and Class IV KDACs where expression is limited to certain tissues. The data suggest that KDACs have both specific and redundant functions. Additionally, the observation of KDAC in different cellular compartments is consistent with the growing number of acetylated proteins found both in the nucleus and the cytoplasm whose functions and stabilities are influenced by KDAC. Despite these advances, there is not yet a good understanding of how the deacetylase activity of KDACs is regulated.

Application of KDACi in cell cultures and animal models has effectively linked enzymatic deacetylation to pathogenesis of cancer as as well as other diseases. The crystal structure of KDAC8 has provided great insight into the KDAC catalytic mechanism and inhibition. In addition, structural and biochemical characterizations of

KDAC8 have established the important players that make up its catalytic machinery, including the divalent metal ion which is required for class I, II and IV KDACs. The metal binding moiety is a feature found in all KDACi to date. Unfortunately, the broad cellular effect, reduced selectivity and potency of the current KDACi limit their utility. Further characterization of the specificity, catalytic mechanism and regulation of KDAC isozymes should facilitate the development of a second generation of improved KDACi.

The overall goal of this research is to elucidate the mechanistic features that govern the molecular recognition properties of lysine deacetylases. Numerous studies have demonstrated broad substrate selectivity of KDACs, yet no rules have been generated to explain this characteristic. We address this shortcoming by evaluating the fundamental role that the divalent metal ion plays in regulating the activity and substrate specificity of KDAC8. Additionally, we aim to biochemically characterize the functional properties of KDAC11, the lone member of Class IV KDACs and one of the least characterized KDAC isozymes. Finally, we probe the role of the internal channel in the product release with the hope of identifying selective inhibitors for KDAC. Progress has been made on the following objectives:

1. Test the metal-dependent substrate specificity of KDAC8 using a library of acetylated peptide substrates.

The deacetylase activity of KDAC8 is dependent on the identity of metal cofactor (Co^{2+}> Fe^{2+} > Zn^{2+}). Furthermore, the loop structure around the metal site in KDAC8 suggests the possibility that the bound metal ion may alter the peptide selectivity of these enzymes. To test this hypothesis, I (in collaboration with the Mrksich Lab at the

University of Chicago) screened the reactivity of KDAC8 with a library of peptides having the sequence GXK(Ac)ZGC, immobilized on an alkane-thiolate monolayer. Matrix-assisted laser desorption ionization time-of-flight mass spectrometry (MALDI TOF MS) spectra of the immobilized peptide substrate before and after incubation with KDAC8 was used to determine KDAC-catalyzed deacetylation. The reactivity of $Zn^{2+}$and Fe^{2+}-KDAC8 resulted in three specificity profiles: peptides that were deacetylated more rapidly by either Zn^{2+}or $Fe^{2+}$and peptides substrates that display similar reactivity with both enzymes. To confirm these specificity profiles, I measured the steady-state kinetic parameters k_{cat}/K_m for peptide substrates represented by each specificity profile. The k_{cat}/K_m values for Fe^{2+}specific peptides demonstrate higher reactivity with Fe^{2+}compared to the Zn^{2+}-bound KDAC8. The peptides characterized as non-specific have similar k_{cat}/K_m values for both enzymes. Together these results show that the substrate specificity of KDAC8 is regulated by divalent metal ion.

2. Probe the substrate selectivity of KDAC11.

KDAC11 has received considerable attention in recent months due to *in vivo* data that suggest a unique role for this enzyme in the immune response. *In vitro* characterization of KDAC11 has been difficult primarily due to low activity in the commonly used assays. I screened the reactivity of KDAC11 with a library of 384 peptides (GXK(Ac)ZGC) using MALDI TOF MS to measure reaction progress. The profile for Co^{2+}–bound KDAC11 resulted in the identification of three rapidly deacetylated peptides (GFK(Ac)LGC, GPK(Ac)LGC, GYK(Ac)LGC). Interestingly, the deacetylated

sequences (GFK(Ac)LGC, GPK(Ac)LGC, GYK(Ac)LGC) resemble a sequence (IIAPPKLAC) located on the N-terminus of Cdt1. Cdt1 is a DNA license replication factor that is proposed to be reversibly deacetylated at an N-terminal site catalyzed by KDAC11. To follow up on this result, we synthesized a longer (IIAPPKLAC) acetylated lysine peptide sequence that matches the sequence motif on the N-terminus of Cdt1. The k_{cat}/K_m for the Zn^{2+}-bound KDAC11 on this sequence is increased by 1333-fold over the commercially available coumarin substrate to a value of $0.33 \pm 0.04\ \mu M^{-1}s^{-1}$. Furthermore, the reactivity of KDAC11 with this sequence varies with the bound divalent metal ions ($Zn^{2+} < Fe^{2+}$), a property also observed in KDAC8.

3. Probe the functional role of an internal cavity in efficient catalytic deacetylation.

Computational and structural methods revealed a conserved Arg37 residue at the center of the internal cavity in KDAC8 and suggested that this side chain plays a key role in the deacetylation catalytic cycle by facilitating dissociation of the acetate product. Substitution of Agr37 with either alanine (R37A) or glutamate (R37E) decreases the value of k_{cat}/K_M by 528-fold for the alanine mutant and 4×10^5-fold for the R37E mutant. The CD spectrum of the R37A KDAC8 mutant is nearly identical to that of WT, indicating that the overall structure is unaffected by deletion of the R37 side chain. Furthermore, Arg37 decreases the affinity of KDAC8 for acetate; the IC_{50} value for inhibition of turnover by acetate is increased by 160-fold in the R37A mutant. Altogether, these results show that R37 is important for stabilizing catalysis and acetate affinity, and could be exploited for preparing specific inhibitors of KDAC8.

Bibliography

1. Walsh, C. T., Garneau-Tsodikova, S., and Gatto, G. J., Jr. (2005) *Angew Chem Int Ed Engl* **44**, 7342-7372

2. Potempa, J. (2012) *Journal of innate immunity* **4**, 119-120

3. Lin, Y. Y., Kiihl, S., Suhail, Y., Liu, S. Y., Chou, Y. H., Kuang, Z., Lu, J. Y., Khor, C. N., Lin, C. L., Bader, J. S., Irizarry, R., and Boeke, J. D. (2012) *Nature* **482**, 251-U149

4. Gurard-Levin, Z. A., Kilian, K. A., Kim, J., Bahr, K., and Mrksich, M. (2010) *ACS Chem Biol* **5**, 863-873

5. ALLFREY, V. G., FAULKNER, R., and MIRSKY, A. E. (1964) *Proceedings of the National Academy of Sciences of the United States of America* **51**, 786-794

6. Marks, P., Rifkind, R. A., Richon, V. M., Breslow, R., Miller, T., and Kelly, W. K. (2001) *Nature Reviews Cancer* **1**, 194-202

7. Pazin, M. J., and Kadonaga, J. T. (1997) *Cell* **89**, 325-328

8. Smith, K. T., and Workman, J. L. (2009) *Nat Biotechnol* **27**, 917-919

9. Minucci, S. (2006) *Nature Reviews Cancer*

10. Norris, K. L., Lee, J. Y., and Yao, T. P. (2009) *Sci Signal* **2**, pe76

11. Kouzarides, T. (2000) *The EMBO journal* **19**, 1176-1179

12. De Ruijter, A. J. M., Van Gennip, A. H., Caron, H. N., Kemp, S., and Van Kuilenburg, A. B. P. (2003) *Biochem J* **370**, 737-749

13. Hayakawa, T., and Nakayama, J. (2011) *J Biomed Biotechnol* **2011**, 129383

14. Gallinari, P., Di Marco, S., Jones, P., Pallaoro, M., and Steinkühler, C. (2007) *Cell research* **17**, 195-211

15. Waltregny, D., Glénisson, W., Tran, S. L., North, B. J., Verdin, E., Colige, A., and Castronovo, V. (2005) *FASEB journal : official publication of the Federation of American Societies for Experimental Biology* **19**, 966-968

16. Haberland, M., Montgomery, R. L., and Olson, E. N. (2009) *Nat Rev Genet* **10**, 32-42

17. Yang, X.-J., and Seto, E. (2008) *Nature reviews. Molecular cell biology* **9**, 206-218

18. Zhang, C. L., McKinsey, T. A., Chang, S., Antos, C. L., Hill, J. A., and Olson, E. N. (2002) *Cell* **110**, 479-488

19. Chang, S., McKinsey, T. A., Zhang, C. L., Richardson, J. A., Hill, J. A., and Olson, E. N. (2004) *Molecular and cellular biology* **24**, 8467-8476

20. Kawaguchi, Y., Kovacs, J. J., McLaurin, A., Vance, J. M., Ito, A., and Yao, T. P. (2003) *Cell* **115**, 727-738

21. Guardiola, A. R., and Yao, T. P. (2002) *The Journal of biological chemistry* **277**, 3350-3356

22. Lahm, A., Paolini, C., Pallaoro, M., Nardi, M. C., Jones, P., Neddermann, P., Sambucini, S., Bottomley, M. J., Lo Surdo, P., Carfi, A., Koch, U., De Francesco, R., Steinkuhler, C., and Gallinari, P. (2007) *Proceedings of the National Academy of Sciences of the United States of America* **104**, 17335-17340

23. Witt, O., Deubzer, H. E., Milde, T., and Oehme, I. (2009) *Cancer letters* **277**, 8-21

24. Gao, L., Cueto, M. A., Asselbergs, F., and Atadja, P. (2002) *The Journal of biological chemistry* **277**, 25748-25755

25. Singh, B. N., Zhang, G., Hwa, Y. L., Li, J., Dowdy, S. C., and Jiang, S.-W. (2010) *Expert review of anticancer therapy* **10**, 935-954

26. Chang, J., Varghese, D. S., Gillam, M. C., Peyton, M., Modi, B., Schiltz, R. L., Girard, L., and Martinez, E. D. (2012) *British journal of cancer* **106**, 116-125

27. Dokmanovic, M., Clarke, C., and Marks, P. A. (2007) *Molecular cancer research : MCR* **5**, 981-989

28. Millar, C. B., Kurdistani, S. K., and Grunstein, M. (2004) *Cold Spring Harbor symposia on quantitative biology* **69**, 193-200

29. Umehara, T., Nakamura, Y., Wakamori, M., Ozato, K., Yokoyama, S., and Padmanabhan, B. (2010) *FEBS Lett* **584**, 3901-3908

30. Umehara, T., Nakamura, Y., Jang, M. K., Nakano, K., Tanaka, A., Ozato, K., Padmanabhan, B., and Yokoyama, S. (2010) *The Journal of biological chemistry* **285**, 7610-7618

31. Riolo, M. T., Cooper, Z. A., Holloway, M. P., Cheng, Y., Bianchi, C., Eakirevich, E., Ma, L., Chin, Y. E., and Altura, R. A. (2012) *The Journal of biological chemistry*

32. de Leval, L., Waltregny, D., Boniver, J., Young, R. H., Castronovo, V., and Oliva, E. (2006) *Am J Surg Pathol* **30**, 319-327

33. Gao, Z., He, Q., Peng, B., Chiao, P. J., and Ye, J. (2006) *The Journal of biological chemistry* **281**, 4540-4547

34. Lf, C., Fischle, W., Verdin, E., and Greene, W. C. (2001) *Science (New York, N.Y.)* **293**, 1653-1657

35. Pickart, C. M., and Cohen, R. E. (2004) *Nature reviews. Molecular cell biology* **5**, 177-187

36. Caron, C., Boyault, C., and Khochbin, S. (2005) *Bioessays* **27**, 408-415

37. Juan, L. J., Shia, W. J., Chen, M. H., Yang, W. M., Seto, E., Lin, Y. S., and Wu, C. W. (2000) *The Journal of biological chemistry* **275**, 20436-20443

38. Ito, A., Kawaguchi, Y., Lai, C. H., Kovacs, J. J., Higashimoto, Y., Appella, E., and Yao, T. P. (2002) *Embo J* **21**, 6236-6245

39. Grönroos, E., Hellman, U., Heldin, C.-H., and Ericsson, J. (2002) *Molecular cell* **10**, 483-493

40. Simonsson, M., Heldin, C. H., Ericsson, J., and Gronroos, E. (2005) *J Biol Chem* **280**, 21797-21803

41. Kijima, M., Yoshida, M., Sugita, K., Horinouchi, S., and Beppu, T. (1993) *The Journal of biological chemistry* **268**, 22429-22435

42. Johnstone, R. W. (2002) *Nature reviews. Drug discovery* **1**, 287-299

43. Rundlett, S. E., Carmen, A. A., Kobayashi, R., Bavykin, S., Turner, B. M., and Grunstein, M. (1996) *Proceedings of the National Academy of Sciences of the United States of America* **93**, 14503-14508

44. Carmen, A. A., Rundlett, S. E., and Grunstein, M. (1996) *The Journal of biological chemistry* **271**, 15837-15844

45. Cole, K. E., Dowling, D. P., Boone, M. A., Phillips, A. J., and Christianson, D. W. (2011) *Journal of the American Chemical Society* **133**, 12474-12477

46. Leggatt, G. R., and Gabrielli, B. (2012) *Immunology and cell biology* **90**, 33-38

47. Finnin, M. S., Donigian, J. R., Cohen, A., Richon, V. M., Rifkind, R. A., Marks, P. A., Breslow, R., and Pavletich, N. P. (1999) *Nature* **401**, 188-193

48. Vannini, A., Volpari, C., Filocamo, G., Casavola, E. C., Brunetti, M., Renzoni, D., Chakravarty, P., Paolini, C., De Francesco, R., Gallinari, P., Steinkühler, C., and Di Marco, S. (2004) *Proceedings of the National Academy of Sciences of the United States of America* **101**, 15064-15069

49. Gattis, S. G., Hernick, M., and Fierke, C. A. (2010) *J Biol Chem* **285**, 33788-33796

50. Hernick, M., and Fierke, C. A. (2005) *Arch Biochem Biophys* **433**, 71-84

51. Ficner, R. (2009) *Current topics in medicinal chemistry* **9**, 235-240

52. Dowling, D. P., Gattis, S. G., Fierke, C. A., and Christianson, D. W. (2010) *Biochemistry* **49**, 5048-5056

53. Wu, R. B., Wang, S. L., Zhou, N. J., Cao, Z. X., and Zhang, Y. K. (2010) *J Am Chem Soc* **132**, 9471-9479

54. Wu, R. B., Hu, P., Wang, S. L., Cao, Z. X., and Zhang, Y. K. (2010) *J Chem Theory Comput* **6**, 337-343

55. Gantt, S. L. (2006) Human Histone Deacetylase 8: Metal Dependence and Catalytic Mechanism. in *Biologican Chemistry*, University of Michigan, Ann Arbor, MI

56. Bottomley, M. J., Lo Surdo, P., Di Giovine, P., Cirillo, A., Scarpelli, R., Ferrigno, F., Jones, P., Neddermann, P., De Francesco, R., Steinkuhler, C., Gallinari, P., and Carfi, A. (2008) *J Biol Chem* **283**, 26694-26704

57. Vallee, B. L., and Falchuk, K. H. (1993) *Physiol Rev* **73**, 79-118

58. Outten, C. E., and O'Halloran, T. V. (2001) *Science* **292**, 2488-2492

59. Gantt, S. L., Gattis, S. G., and Fierke, C. A. (2006) *Biochemistry* **45**, 6170-6178

60. Auld, D. S. (2001) *Biometals* **14**, 271-313

61. Morris, P. (1970) *Journal of Inorganic and Nuclear Chemistry* **32**, 2891-2897

62. Sigel, H. (1970) *Accounts of chemical research*

CHAPTER II

METAL-ION DEPENDENT SUBSTRATE SPECIFICITY OF KDAC8

Introduction

Protein lysine acetylation is catalyzed by lysine acetyl transfereases (KATs) while lysine deacetylases (KDACs) catalyze removal of the acetyl moiety. The balance of the enzymatic activities of KDACs and KATs plays a fundamental role in the stability and function of many proteins in mammalian cells, including histones, p53, and α-tubulin(1). KATs mediated acetylation of histones enhances the binding of transcriptional activators to DNA and facilitates gene transcription; while the removal of the acetyl group by KDACs generally suppresses gene transcription by promoting the formation of a condensed chromatin state. Numerous studies have demonstrated that aberrant KDAC expression is directly correlated with oncogenic transformation. Consequently, inhibitors targeting KDACs have been tested for effects on growth differentiation, apoptosis, and, more recently, neurodegenerative disorders like Parkinson disease. Furthermore, the FDA has approved two broad-spectrum KDAC inhibitors (KDACi), suberoylanilide hydroxamic acid (SAHA) and romidepsin for the treatment of cutaneous T-cell lymphoma (Table 1.1)(2-4). The list of proteins modified by acetylation/deacetylation is

rapidly growing and includes many proteins that operate in diverse cellular processes such as gene regulation, signaling cascades and the unfolded protein response (UPR)(5,6).

Studies, fueled primarily by drug discovery, have identified 18 different isoforms of KDACs. Eleven KDACs require a divalent metal ion for catalytic activity(7). The metal-dependent KDAC family is subdivided into three classes based on sequence homology and cellular localization(8). Class I enzymes (KDAC 1-3, KDAC8) are ubiquitously expressed and are homologous to yeast deacetylase RPD3. Class II (4-7,9-10) KDACs tend to have distinct cellular expression patterns and shuttle between the cytoplasm and the nucleus. Furthermore, these isozymes have homology to yeast deacetylase HDAC1. Last, KDAC11 is the sole member of class IV, which is closely related to the class I enzymes and is highly enriched in brain, heart, and muscle tissues(9). Deciphering the precise biological function of each KDAC is an important aim of many current studies. Nonetheless, it is likely that KDACs have specific as well as redundant biological functions(10). Particularly, a substrate can be processed by one specific KDAC or multiple KDACs depending on the cellular condition.

These deacetylation patterns can be observed, for example, in endothelial cells where KDAC7 is specifically expressed during embryogenesis, and deletion of KDAC7 results in embryonic mice lethality(11). Conversely, broad substrate specificity and redundant function are highlighted by the ubiquitous expression of Class I enzymes(12,13). KDAC8 is ubiquitously expressed in normal human tissues and is found in both the nucleus and the cytoplasm(14). Nuclear fractionation of human colon cancer cell lines indicates that KDAC8 is highly expressed and located in the nucleus. This

implicates KDAC8 in the regulation of transcription likely by deacetylation of histone proteins and provides a rationale for the deleterious effects that sustained expression of KDAC8 has in tumor cells. However, in normal human tissues, KDAC8 is located in the cytoplasm; coimmunoprecipitation experiments in NIH3T3 cells have demonstrated that KDAC8 interacts with α-actin and possibly modulates cytoskeleton contraction(15-18). Additionally, α-actin can be acetylated near the N-terminus and this modification can alter the interaction with myosin. Hence, KDAC8 could alter the actin and myosin association through deacetylation(19,20). Similar to KDAC8, KDAC6 acts on both nuclear and cytoplasmic substrates(21,22). This shuttling capability greatly increases the substrate pool for these enzymes. Accordingly, the molecular recognition of these substrates by KDACs is important to ensure proper cellular function. Likewise the active site structure of KDACs should play a crucial role in molecular recognition of KDACs substrates.

The crystal structures of histone deacetylase like protein (HDLP) and KDAC8 provided the first models for derivation of a general KDAC catalytic mechanism(23,24). These crystal structures revealed a single catalytic Zn^{2+} ion and two bound K^+ ions. The two bound K^+ ions modulate the activity of KDAC8 with one K^+ activating catalytic activity and a second site inhibiting activity(25). Mutagenesis studies indicate that binding to the K^+ site that is 7 Å away from the active site inhibits the activity, suggesting that the binding to the distal K^+ site activates catalysis likely through stabilization. The activating of K^+ also enhances the affinity of KDAC8 for SAHA by 5-fold. Additionally, the regulation of KDAC8 by K^+ ions could play a significant role in modulating gene expression. Hamon et. al showed that bacterial infection of a cell increases the

deacetylation of Histone H4 and this effect is activated K^+ efflux from the cell. These results suggest that the intracellular level of K^+ ions is regulated by the activity of KDAC(26).

The catalytic Zn^{2+} is essential in the mechanism of KDAC8 as it promotes catalysis. Specifically, the catalytic metal-ion decreases the pK_a of the coordinated water molecule and properly orients this water for the efficient nucleophilic attack on the carbonyl carbon of the acetylated substrate (Scheme 1.2)(27). Furthermore, the divalent metal is proposed to coordinate the carbonyl oxygen of the acetylated group in the ground state to enhance the electrophilicity and hence the reactivity of the carbonyl carbon of the acetylated lysine in the substrate. Additionally, the metal ion interaction stabilizes the formation of the oxyanion in the tetrahedral intermediate and the adjoining transition state. Hence, a general acid / general base mechanism was proposed for KDACs. KDAC8 was originally proposed to use Zn^{2+} as a metal cofactor since this metal co-purified with the enzyme and was visualized in the first crystal structure. However, studies have demonstrated that Co^{2+}, $Zn^{2+}$and Fe^{2+} activate KDAC8 and there are now structures of KDAC with bound Fe^{2+}, Co^{2+} and Zn^{2+}(28-30). Additionally, KDAC8 is inhibited by excess zinc, which is a common property of many mononuclear metalloenzymes; biochemical experiments show that KDAC8 is maximally active with a single bound metal ion(31). The value of k_{cat}/K_m for Co^{2+}-substituted KDAC8 is almost 4-fold more active than the Fe^{2+}-substituted enzyme and 9-fold higher than the Zn^{2+}-substituted KDAC8. Also, the identity of the divalent metal ions alters the affinity of inhibitors. The SAHA inhibition constant (K_i) for Zn^{2+}-bound KDAC8 is 2-fold larger than for Fe^{2+}-bound KDAC8 and 5-fold higher than for the Co^{2+}bound enzyme. Additionally, metal

affinity experiments demonstrate that zinc affinity of KDAC8 is pM which is $10^{\wedge 6}$-fold higher than the iron(30). Despite this, since in the cell the free concentration of Zn^{2+} is estimated as many orders of magnitude lower than the free concentration of Fe^{2+} (10-400pM vs 0.2-0.6 μM), it is possible that KDAC8 could be activated by either Zn^{2+} and Fe^{2+} *in vivo*. Considering that iron and zinc are the most abundant trace metals found in humans (0.2-0.5 mM) and these metals are essential co-factors for many enzymes(32), one of these as the bound catalytic metal could play an important role in the function and possible substrate specificity of KDACs.

Here we examine the role the catalytic metal ion in KDACs on the catalytic activity and substrate specificity. KDAC8 is the best characterized isozyme among all the metal-dependent KDACs and not normally found in large protein complexes. We therefore chose to use KDAC8 as a model system for probing the role of metal ions in substrate selectivity. We first measured the reactivity of Zn^{2+} and Fe^{2+} bound KDAC8 with a library of acetylated lysine peptide substrates demonstrating significant alterations in the substrate selectivity. We then measured the effects of metal variation on the Steady state kinetic parameters for the deacetylation of individual peptides using a new assay that measures acetate production. These data confirm that Zn^{2+}/Fe^{2+} metal substitution alters the substrate selectivity of KDAC8. Furthermore, metal switching may be a novel method of regulating KDAC activity and specificity in cells.

Materials and Methods

Expression and Purification

The sequence for the KDAC8 gene was subcloned and put the gene expression under the control of a T7 RNA polymerase promoter into a pET-20b derived expression plasmid which added a C-terminal TEV-His_6 tag (pHD4). After transforming the plasmid into the BL21(DE3) strain of *E. coli*, one colony was inoculated into 5 mL of 2X-YT medium supplemented with 0.1 mg/ml ampicillin and incubated for 4 h at 37°C . The starter culture was used to inoculate 6 L of 2X-YT medium supplemented with 0.1 mg/ml ampicillin and incubated at 37°C until OD_{600} = 0.6-0.7, and then the temperature was reduced to 25 °C for 45 min. Protein synthesis was induced by the addition of 0.5 mM isopropyl β-D-1-thiogalactopyranoside (IPTG) and the cells were incubated for an additional 12-15 hours at 25 °C. The cells were harvested by centrifugation, resuspended in buffer A (30 mM HEPES, 150 mM NaCl, 0.5 mM imidazole, pH 8.0), lysed using a microfluidizer and the resulting extract was clarified by centrifugation (15000 rpm, 40 min, 4 °C). The cell extract was loaded onto a 10 mL metal affinity resin (GE Healthcare, Chelatin Fast Flow Sepharose) column charged with 150 mM nickel chloride. The column was washed with Buffer A containing 25 mM imidazole and then the protein was eluted with Buffer A containing 250 mM imidazole. The His_6-TEV tag was removed by incubation with recombinant TEV protease (100:1, protease: fusion protein) at 4°C and KDAC8/TEV protease then dialyzed overnight in buffer A containing 1 mM tris(2-carboxyethyl) phosphine (TCEP). The nickel column step was ran a second time and the

cleaved KDAC8 was obtained in the flow through. 1-2 mg of > 98% pure KDAC8 was obtained per liter of 2 XYT medium using this protocol.

Apo-KDAC8

Metal-free KDAC8 was prepared by dialyzing the purified enzyme twice overnight against 25 mM 4-morpholinepropanesulfonic acid (MOPS), 1 mM EDTA, and 10 mM dipicolinic acid (DPA), pH 7.5, followed by dialysis against 25 mM MOPS, and 1 μM EDTA, pH 8.0. The enzyme was then concentrated using an Amicon Ultra Microcon centrifugal filtration device (10,000 MWCO) and the buffer was exchanged using a PD-10 gel filtration column (GE Healthcare) equilibrated with 25 mM MOPS, pH 8.0 (pretreated with metal chelating resin, Chelex 100). The metal content of the protein was determined by inductively coupled plasma emission mass spectroscopy (ICP-MS) (Department of Geological Sciences, University of Michigan). The final concentration of KDAC8 was determined by both OD_{280} (ε_{280} =52120 $M^{-1}cm^{-1}$, under denaturing conditions) and the absorbance change after reaction with 5,5'-dithiobis(2-nitrobenzoic acid) (ε_{412} =13,600 $M^{-1}cm^{-1}$).

Mass Spectrometric Assay

Peptide library studies were performed using an assay where 384 acetylated peptides were immobilized on alkenothiolate monolayer that presents a maleimide group. Matrix-assisted laser desortion ionization time-of-flight mass spectrometry (MALDI TOF MS) spectra are taken of the immobilized peptide substrate before and after treatment with KDAC8 (Figure 1). To form the immobilized peptide library, 3 μL of the cysteine-terminated peptides were transferred to each well to react with the maleimide moiety at

37˚C for 1 h. KDAC8 was reconstituted with either Zn^{2+}, Fe^{2+}, and Co^{2+}, in the assay buffer (25 mM Tris, 147 mM NaCl, 10 mM KCl pH 8.0) and incubated on ice for 1 h. The plates were washed with ethanol/water/ethanol followed by reaction with KDAC8 (0.5 μM) at 30 ˚C for 30 min. KDAC8 was stopped with additional ethanol/water/ethanol rinses and the plates were dried under nitrogen gas. A matrix (2,4,6-trihydroxyacetophenone, 25 mg/mL in acetone) was applied to each plate and then air-dried. The plate was loaded onyo the 4800 MALDI mass spectrometer (Applied Biosystems) where a spectrum was obtained.

Acetate assay

An assay that couples the formation of the product acetate to an increase in NADH, as measured by fluorescence (Scheme 1), was used to measure the steady-state kinetic parameters for catalytic deacetylation of peptides without the 4-methyl coumarin (MCA) fluorophore. This assay couples three enzymatic reactions. The first enzyme catalyzes the reaction of acetate with adenosine-5'-triphosphate (ATP) and Coenzyme A (CoA) to form Acetyl-CoA ADP and P_i. In the second step, Acetyl-CoA reacts with oxaloacetate, catalysed by citrate synthase, to produce citrate and CoA. Oxaloacetate is produced from the reaction of malate and NAD to form oxaloacetate and NADH, catalysed by malate dehydrogenase Thus, the consumption of oxaloacetate by the reaction with AcCoA produces an increase in NADH concentration which is monitored at λ_{ex} = 340 nm and λ_{em} = 460 nm. Steady-state kinetic parameters were determined from initial rate reactions (10 μL total) containing 0.5 μM KDAC8 apo or metal bound, and varying peptides concentrations (5-400 μM). Apo KDAC8 was incubated with equimolar

concentration of Fe^{2+} and Zn^{2+} in 25 mM Tris, 147 mM NaCl, and 10 mM KCl pH8 for 30 min prior to initiating the reaction with peptides. The reactions were stopped by addition of 0.1% HCl and neutralized with 1% sodium bicarbonate to a final volume to 10 µL prior to detection of acetate using the coupled assay. For acetate detection, the enzymes and substrates were purchased from R-Biopharma and mixed according to the instructions. 8µl of neutralized solution deacetylase reaction was added to 60 µL of coupled enzyme reaction mixture for 30 min prior to loading onto a 96 well plate (Half Area Black Flat Bottom Polystyrene non-binding surface, Corning) and measurement of the fluorescence read on a plate reader (BMG Latech, FLUOstar Galaxy). Amount of product was determined from a standard curve calculated using known concentrations of acetate.

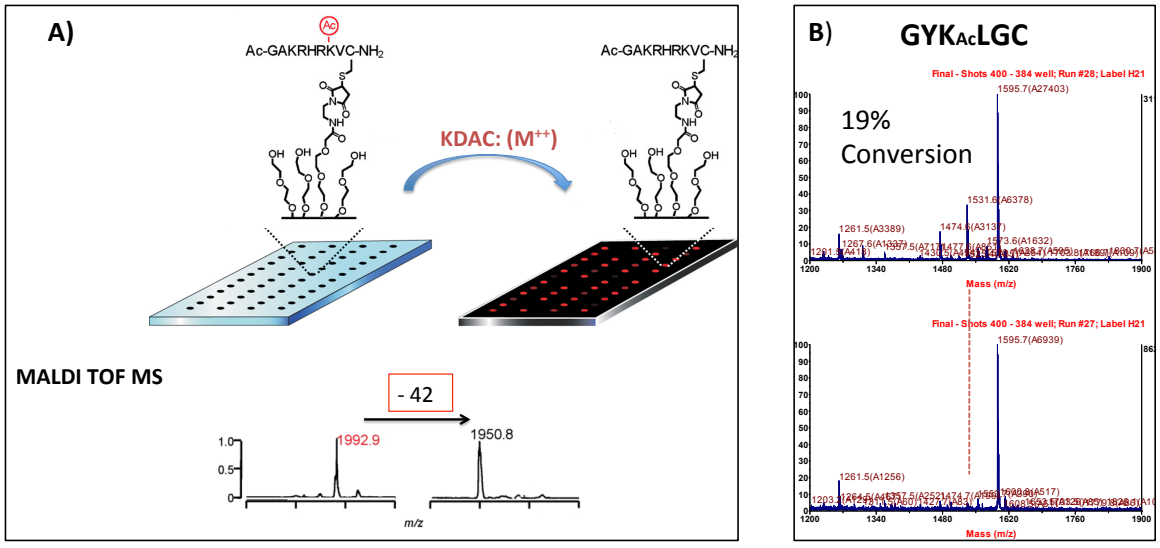

Figure 2.1. Mass Spectrometric Assay. A) Immobilized peptide substrates are incubated with the enzyme and loaded on a MALDI mass spectrometer. B) A sample spectrum showing a 19% deacetylation calculated from equation 1 (substrate peak on top, substrate and product peak bottom)

% deacetylation = Product (AUC) / (Product (AUC) + Substrate (AUC) **Equation 1**

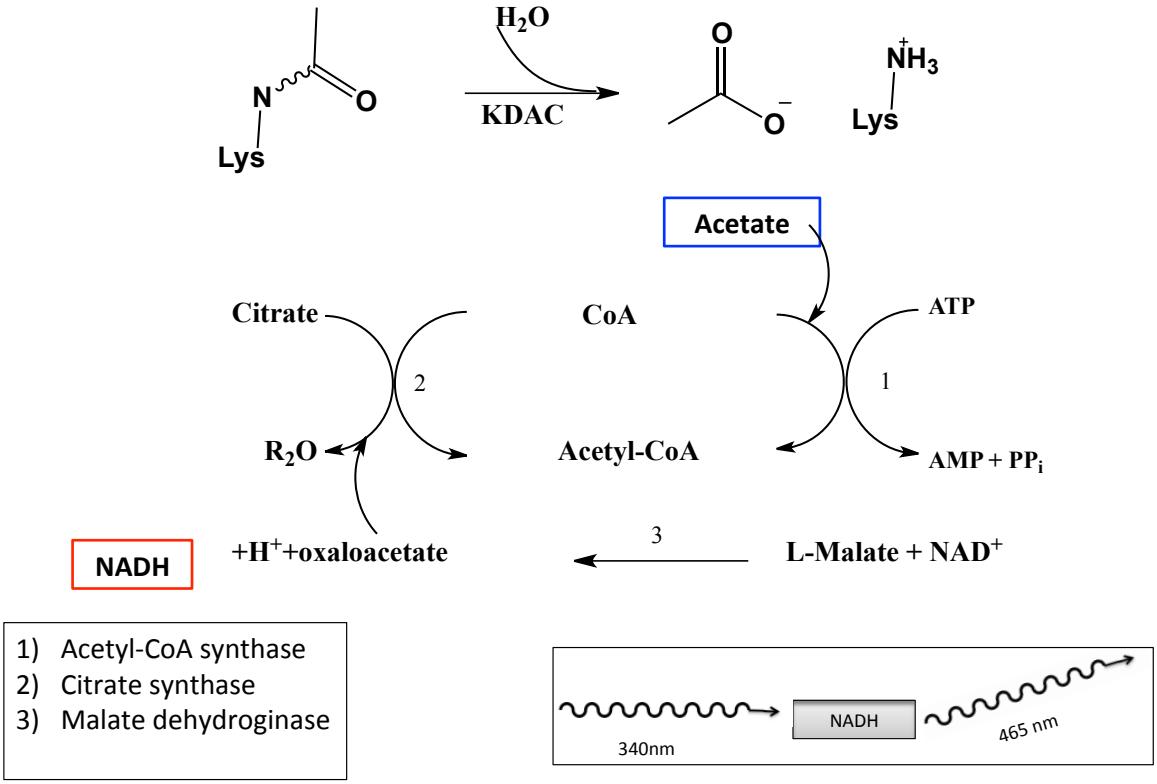

Scheme 2.1. Acetate Assay. Scheme showing the reactions that couple the increase of the acetate product to an increase in NADH fluorescence.

Results

Substrate selectivity of metal-bound KDAC8

To evaluate whether the identity of the active site metal ion in KDA8 affects the substrate selectivity, I prepared KDAC8 containing either a stoichiometrically bound Fe^{2+} or Zn^{2+} metal cofactor and reacted these enzymes with a peptide library (in collaboration with the Mrksich Lab, University of Chicago). This library consists of 384 acetylated lysine peptides with the sequence (GXK(ac)ZGC) randomized at X and Z. The cysteine residue in the peptide was reacted to a maleimide-terminated monolayer. Matrix-assisted laser desorption ionization time-of-flight mass spectrometry (MALDI TOF MS) spectra were obtained of the immobilized peptide substrate before and after incubation with the enzyme for 30 min at 37°C. The fraction of deacetylation was calculated from area of the deacetylated peak (area under the curve (AUC)) divided by the combined areas of both peaks (Equation.1) (this assumes a similar ionization efficiency for both)(33). For the Zn^{2+}-KDAC8 the fraction deacetylated ranged from (3%-93%) (Figure 2.2a). The reactivity can be divided into three groups: 1) inactive, < 3% deacetylation, 195 peptides); 2) moderate activity, 72 peptides, (3-15%) deacetylated; and 3) high activity, >15%, 117 peptides.

Similarly, the Fe^{2+}-substituted KDAC8 has three reactivity profiles (Figure 2.2a). 1) low activity ranged from (0-3 % deactylation, 161 peptides); 2) 62 peptides had moderate activity (3-15 %); and 3) 160 peptides had high activity that ranged from 15-77%.

It was really apparent from the specificity grids (Figure 2.2c) that KDAC8 selectivity alters with the active site metal ion. Ratios of the fraction deacetylated catalyzed by the

Fe^{2+}-KDAC8 to Zn^{2+}-KDAC8 clearly demonstrate the existence of these specificity profiles.

1) 40 peptides have higher activity with Zn^{2+}-KDAC8 than Fe^{2+} KDAC8 (Zn/Fe > 7)
2) 51 peptides are more reactive with Fe^{2+} KDAC8 (Fe/Zn >7)
3) 120 peptides have comparable activity with both metals substituted enzymes (2<Fe/Zn<2)
4) 173 peptides react with neither

Overall, these results show broad activity within the library. In general, non-specific substrates tend to prefer a Phe at the X-position when Z can vary. The Zn^{2+} specific pool likes an aromatic at the Z-position and the Fe^{2+} peptides select for negatively charged residues at the X-position. The largest number of peptides has comparable reactivity with both Zn^{2+} and Fe^{2+}-substituted KDAC8. This would be consistent with the notion that KDAC8 would have many substrates *in vivo* and that it uses either iron or zinc to deacetylate substrates. Finally, the specific profiles indicate that the bound metal ion dictates a conformation in the overall protein structure that gives the enzyme substrate specificity.

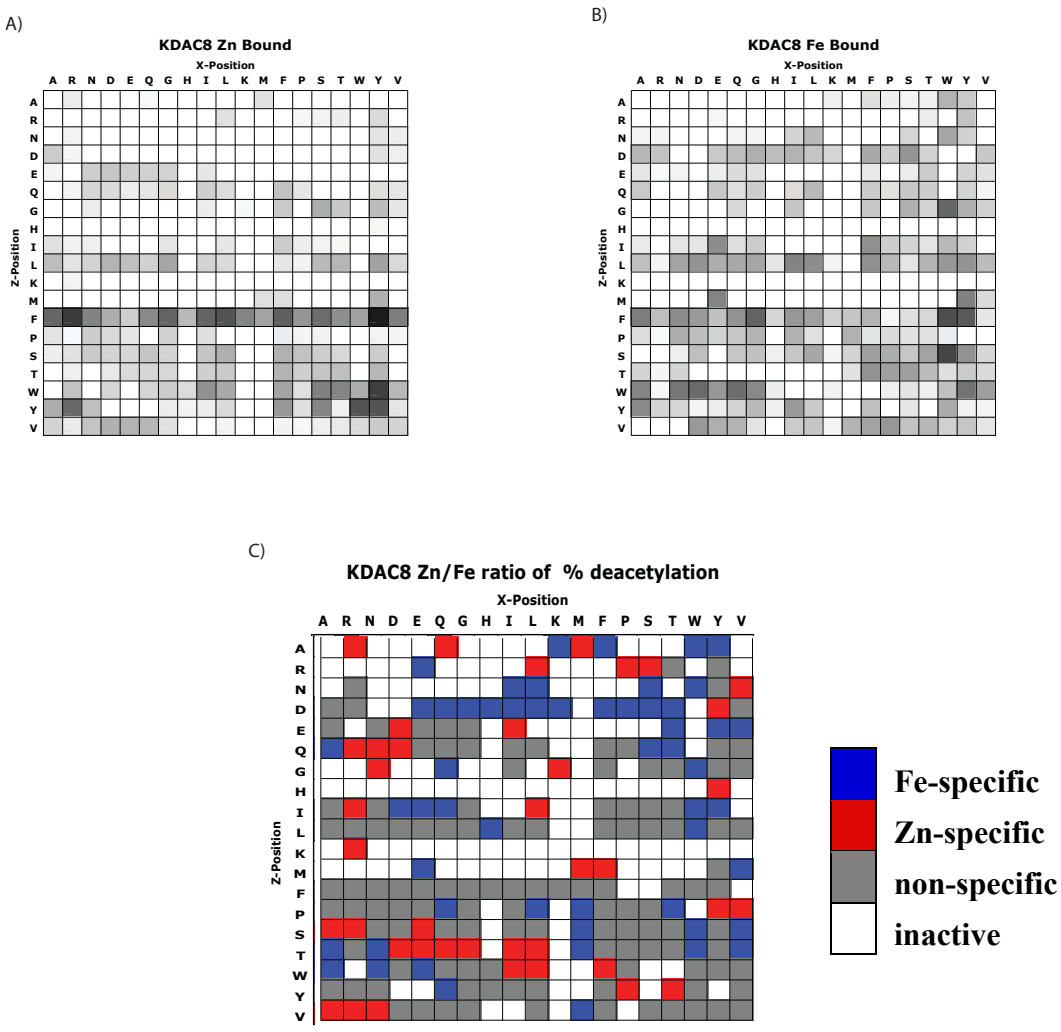

Figure 2.2. Fe^{2+} and Zn^{2+}-bound KDAC8 substrate selectivity profiles G**X**K(Ac)**Z**GC peptide library (X and Z represent all AAs except Cys). 0.5 µM KDAC8. Buffer: 50 mM TRIS pH8, 147 mM NaCl, 3 mM KCl, 30 °C for 1 h. A) Zn^{2+}-bound KDAC8 reactivity B) Fe^{2+}-bound KDAC8 reactivity C) KDAC8 metal specificity % deacetylation calculated for Zn^{2+} peptides was divided by % deacetylation for Fe^{2+}.

Zn^{2+}-HDAC8: High Selectivity, high activity

Mass	G**X**K(Ac)**Z**GC			
	Z	**X**	**% Zn activity**	**% Fe activity**
691	E	D	24	
659	V	L	20	
746	W	L	36	

Fe^{2+}-HDAC8: High selectivity, high Activity

Mass	G**X**K(Ac)**Z**GC			
	Z	**X**	**% Fe activity**	**% Zn activity**
675	L	D	44	
747	W	N	57	
697	S	Y	51	10

Low metal selectivity, high activity

Mass	G**X**K(Ac)**Z**GC			
	Z	**X**	**% Zn activity**	**%Fe activity**
665	F	A	64	54
750	F	R	81	28
708	F	N	52	48

Table 2.1. Peptides selected for multiple turnover kinetics. Selection was based on high activity and metal specificity.

Kinetic constants of KDAC8 substrates

To further explore the metal-dependent substrate selectivity, I conducted assays in solution to obtain the steady-state kinetic parameters, k_{cat}/Km. I selected 9 peptides substrates with varying selectivity profiles to analyze based on the selectivity trends previously identified and the Mrksich lab synthesized these peptides. (Table 2.1) I used an optimized KDAC assay that measures the production of acetate from the appearance of NADH using a coupled assays system (see M&M). I used this assay to measure the kinetic parameter k_{cat}/K_m. The results are listed in table 2.2. In essence, the Fe^{2+}, Zn^{2+}, and non-specific profiles were reproduced using the acetate assay. . The k_{cat}/K_m values for Fe^{2+}specific candidates were higher for Fe^{2+}-bound KDAC8 compared to the Zn^{2+} substituted enzyme. The non-specific pool retains its characteristic. For the Zn^{2+}specific pool, the k_{cat}/K_m values were higher for Zn^{2+}-bound KDAC8; however, the K_m values were slightly lower for the Fe^{2+}-bound KDAC8, which suggest that the conditions seen on the plate may have been k_{cat}. Together these results show that the substrate specificity of KDAC8 is regulated by the bound metal ion.

GXK(Ac)ZGC		Zn^{2+}-reactivity			Fe^{2+}-reactivity			Zn/Fe Ratio
Z	**X**	k_{cat}/K_m ($\mu M^{-1}S^{-1}$)	k_{cat} (S-1)	K_m (μM)	k_{cat}/K_m ($\mu M^{-1}S^{-1}$)	k_{cat} (S-1)	K_m (μM)	(k_{cat}/K_m)
Zn^{2+}-specific								
E	D	0.18 ± 0.04	0.61 ±0.02	3.5 ± 1	0.09 ± 0.02	1.8 ± 0.1	19 ± 5	2
V	L	0.053 ± .027	0.37 ±0.04	7 ± 4	0.031 ± 0.009	1.45 ± 0.14	47 ± 18	1.7
W	L	0.0886 ± 0.03	0.34 .01	3.92 ± 1.4	0.0049 ± .001	0.4 ± 0.05	82 ± 30	18
Fe^{2+}-specific								
L	D	0.02 ± 0.01	0.158 ± 0.02	7.7 ± 4.5	0.13 ± 0.03	1.41 ± 0.12	11 ± 3.7	0.15
S	Y	0.09 ± 0.14	0.24 ± 0.05	2.6 ± 4.3	0.34 ± 0.11	1.16 ± 0.06	3.4 ± 1.2	0.33
L	W	n.d.[a]	n.d.[a]	n.d.[a]	0.1299 ± .03	1.44 ± 0.12	11.08 ± 3.7	<0.1
Non-specific								
F	A	0.130 ± 0.002	0.45 ± 0.03	34 ± 8.6	.0139 ± 0.001	0.608 ± .02	43 ± 5.3	0.9
F	R	0.0111 ± 0.0029	2.4 ± 0.4	220 ± 90	0.0127 ±0 .0015	2.92 ± .21	228 ± 43	0.8
F	N	0.024 ± 0.009	0.36 ± 0.03	15 ± 6	0.044 ± 0.021	1.0 ± 0.1	23 ± 13	0.6

Table 2.2. Steady State Kinetic parameters for Zn^{2+} and Fe^{2+} -bound KDAC8. Kinetic rate parameters, k_{cat}/K_m, k_{cat}, and K_m were determined from initial velocities measured from changes in NADH fluorescence and fitted to the Michealis-Menten equation. [a] initial velocities could not be determined

Discussion

KDAC8 is one of the best-characterized KDAC isozyme and is a great platform to study the regulation of substrate specificity of KDACs in general. Several studies have shown that the activity of KDAC8 is dependent on the modification state (methylation, acetylation) of the substrate(34,35). Few studies have addressed how the identify of the catalytic metal ion bound to KDACs affects their activity and substrate recognition. Recent studies have demonstrated that both Fe^{2+} and Zn^{2+} activate KDAC8 and both metal ions alter the reactivity of KDAC8 on the commercially available coumarin substrate(29). We used peptide library studies showing that Zn^{2+} and Fe^{2+} activate deactylation of a wide variety of peptide sequences and that the selectivity depends on the identity of the metal cofactor. Iron and zinc are the most abundant metals in mammalian cells. Based on high activity, it seems feasible that KDAC8 could use either of these metals to activate catalysis *in vivo*. The broad substrate selectivity observed in both the Fe^{2+} and Zn^{2+} profiles indicate that KDAC8 has the potential to catalyze the deacetylation of many substrates in the cell. There are only 18 KDACs to potentially catalyze the deacetylation of more than 3000 members of the acetylome(36,37). Consequently, regulation of the KDAC activities could be vital for maintaining optimal cellular processes.

The crystal structure of KDAC8 indicates that the substrate binding site is lined abundantly by loops (Figure 1.3a)(38). Furthermore, the residues that coordinate the active site metal are also positioned by the loops in KDAC8. These observations suggest that intrinsic properties of the metal ion, particularly Lewis acidity, ligands coordination

geometry and ligation kinetics, could dictate a specific (39)conformation in the overall protein structure(40,41). Consequently, this specific conformation would largely govern the molecular recognition of KDAC8.

The metal-dependent substrate specificity of KDAC8 could depend on availability of each metal. Under cellular conditions such as redox stress, the concentration of Zn^{2+} is increased as cellular zinc ligands, which are frequently cysteine residues, get oxidized and release Zn^{2+}(42). Under these conditions, the Zn^{2+} concentration can increase from pM to nM(43). The dependence of Fe^{2+} concentration on the redox state of the cell is unclear, although it is reasonable to assume that it might decrease. Hence, KDACs could substitute Zn^{2+}, a redox inert catalytic metal, to maintain their function and to alter substrate selectivity. Furthermore, pull-down experiments with LpxC, a metal dependent bacterial deacetylase, demonstrate that this deacetylase adapts to its cellular environment when it switches Zn^{2+} for Fe^{2+} under aerobic condition where the concentration of Zn^{2+} was high compared to Fe^{2+}(44). Hence, it is plausible to assume that KDACs would have a similar mechanism where they operate with the divalent metal that is most abundant.

The specificity profile results obtained on the mass spectrometry plates were largely reproduced in solution assays. The non-specific pool of substrate had similar catalytic efficiency indicating that metal ions do alter the binding and catalysis of these substrates. Fe^{2+} and Zn^{2+} specific peptides also retained their identity. A difference can be observed in the ratio of %deacetylation (Fe/Zn), which is much larger on the plates compared to data obtained in the acetate assay (Table 2.2). It is very possible that the conditions seen on the arrays plate were under saturating substrate concentration and that

accounts for the biggest difference the between calculated %deacetylation of Fe^{2+} and Zn^{2+}.

In summary, the study presents the first demonstration that the substrate specificity of KDAC varies with the identity of the active site metal ion. The enormous number of acetylated proteins in mammalian cells indicates that each KDAC has more than one substrate. If so, normal cells likely maintain a strict regulation of these KDACs. Several studies have addressed the regulation of KDACs by the modification state of the substrate, such as competition between acetylation, methylation, and ubiquitination. Additionally, KDACs can be post-transnationally modified. The peptide library studies here show that KDAC8 has metal-dependent substrate specificity. These data also establish KDAC8 as both an Fe^{2+} and Zn^{2+} enzyme and provide a fundamental model for the regulation of KDACs in mammalian cells.

BIBLIOGRAPHY

1. Haberland, M., Montgomery, R. L., and Olson, E. N. (2009) *Nat Rev Genet* **10**, 32-42

2. Yang, X.-J., and Seto, E. (2008) *Nature reviews. Molecular cell biology* **9**, 206-218

3. Singh, B. N., Zhang, G., Hwa, Y. L., Li, J., Dowdy, S. C., and Jiang, S.-W. (2010) *Expert review of anticancer therapy* **10**, 935-954

4. Sengupta, N., and Seto, E. (2004) *Journal of cellular biochemistry* **93**, 57-67

5. Kahali, S., Sarcar, B., and Chinnaiyan, P. (2011) *Methods in enzymology* **490**, 159-174

6. Grönroos, E., Hellman, U., Heldin, C.-H., and Ericsson, J. (2002) *Molecular cell* **10**, 483-493

7. Witt, O., Deubzer, H. E., Milde, T., and Oehme, I. (2009) *Cancer letters* **277**, 8-21

8. De Ruijter, A. J. M., Van Gennip, A. H., Caron, H. N., Kemp, S., and Van Kuilenburg, A. B. P. (2003) *Biochem J* **370**, 737-749

9. Gao, L., Cueto, M. A., Asselbergs, F., and Atadja, P. (2002) *The Journal of biological chemistry* **277**, 25748-25755

10. Heltweg, B., Dequiedt, F., Marshall, B. L., Brauch, C., Yoshida, M., Nishino, N., Verdin, E., and Jung, M. (2004) *Journal of medicinal chemistry* **47**, 5235-5243

11. Chang, S., Young, B. D., Li, S., Qi, X., Richardson, J. A., and Olson, E. N. (2006) *Cell* **126**, 321-334

12. Taunton, J., Hassig, C. A., and Schreiber, S. L. (1996) *Science* **272**, 408-411

13. Yang, X. J., and Seto, E. (2003) *Curr Opin Genet Dev* **13**, 143-153

14. Waltregny, D., de Leval, L., Glénisson, W., Ly Tran, S., North, B. J., Bellahcène, A., Weidle, U., Verdin, E., and Castronovo, V. (2004) *The American journal of pathology* **165**, 553-564

15. Van den Wyngaert, I., de Vries, W., Kremer, A., Neefs, J., Verhasselt, P., Luyten, W. H., and Kass, S. U. (2000) *FEBS Lett* **478**, 77-83

16. Oehme, I., Deubzer, H. E., Wegener, D., Pickert, D., Linke, J.-P., Hero, B., Kopp-Schneider, A., Westermann, F., Ulrich, S. M., von Deimling, A., Fischer, M., and Witt, O. (2009) *Clinical Cancer Research* **15**, 91-99

17. de Leval, L., Waltregny, D., Boniver, J., Young, R. H., Castronovo, V., and Oliva, E. (2006) *Am J Surg Pathol* **30**, 319-327

18. Durst, K. L., Lutterbach, B., Kummalue, T., Friedman, A. D., and Hiebert, S. W. (2003) *Molecular and cellular biology* **23**, 607-619

19. Abe, A., Saeki, K., Yasunaga, T., and Wakabayashi, T. (2000) *Biochemical and biophysical research communications* **268**, 14-19

20. Karolczak-Bayatti, M., Sweeney, M., Cheng, J., Edey, L., Robson, S. C., Ulrich, S. M., Treumann, A., Taggart, M. J., and Europe-Finner, G. N. (2011) *The Journal of biological chemistry* **286**, 34346-34355

21. Namdar, M., Perez, G., Ngo, L., and Marks, P. A. (2010) *Proceedings of the National Academy of Sciences of the United States of America* **107**, 20003-20008

22. Riolo, M. T., Cooper, Z. A., Holloway, M. P., Cheng, Y., Bianchi, C., Eakirevich, E., Ma, L., Chin, Y. E., and Altura, R. A. (2012) *The Journal of biological chemistry*

23. Finnin, M. S., Donigian, J. R., Cohen, A., Richon, V. M., Rifkind, R. A., Marks, P. A., Breslow, R., and Pavletich, N. P. (1999) *Nature* **401**, 188-193

24. Vannini, A., Volpari, C., Filocamo, G., Casavola, E. C., Brunetti, M., Renzoni, D., Chakravarty, P., Paolini, C., De Francesco, R., Gallinari, P., Steinkühler, C., and Di Marco, S. (2004) *Proceedings of the National Academy of Sciences of the United States of America* **101**, 15064-15069

25. Gantt, S. L., Joseph, C. G., and Fierke, C. A. (2010) *J Biol Chem* **285**, 6036-6043

26. Hamon, M. A., and Cossart, P. (2011) *Infect Immun* **79**, 2839-2846

27. Hernick, M., and Fierke, C. A. (2005) *Arch Biochem Biophys* **433**, 71-84

28. Gantt, S. L., Gattis, S. G., and Fierke, C. A. (2006) *Biochemistry* **45**, 6170-6178

29. Gantt, S. L. (2006) Human Histone Deacetylase 8: Metal Dependence and Catalytic Mechanism. in *Biologican Chemistry*, University of Michigan, Ann Arbor, MI

30. Dowling, D. P., Gattis, S. G., Fierke, C. A., and Christianson, D. W. (2010) *Biochemistry* **49**, 5048-5056

31. Maret, W., Yetman, C. A., and Jiang, L. (2001) *Chemico-biological interactions* **130-132**, 891-901

32. Outten, C. E., and O'Halloran, T. V. (2001) *Science* **292**, 2488-2492

33. Gurard-Levin, Z. A., Kilian, K. A., Kim, J., Bahr, K., and Mrksich, M. (2010) *ACS Chem Biol* **5**, 863-873

34. Gurard-Levin, Z. A., and Mrksich, M. (2008) *Biochemistry* **47**, 6242-6250

35. Riester, D., Hildmann, C., Grünewald, S., Beckers, T., and Schwienhorst, A. (2007) *Biochemical and biophysical research communications* **357**, 439-445

36. Norris, K. L., Lee, J.-Y., and Yao, T. P. (2009) *Sci Signal* **2**, 76

37. Smith, K. T., and Workman, J. L. (2009) Introducing the acetylome. in *Nat Biotechnol*

38. Vannini, A., Volpari, C., Gallinari, P., Jones, P., Mattu, M., Carfí, A., De Francesco, R., Steinkühler, C., and Di Marco, S. (2007) *EMBO reports* **8**, 879-884

39. Maret, W. (2006) *Antioxidants & redox signaling* **8**, 1419-1441

40. Auld, D. S. (2009) *Biometals : an international journal on the role of metal ions in biology, biochemistry, and medicine* **22**, 141-148

41. Auld, D. S. (2001) *Biometals : an international journal on the role of metal ions in biology, biochemistry, and medicine* **14**, 271-313

42. Maret, W., and Krezel, A. (2007) *Molecular medicine (Cambridge, Mass.)* **13**, 371-375

43. Maret, W. (2009) *Biometals : an international journal on the role of metal ions in biology, biochemistry, and medicine* **22**, 149-157

44. Gattis, S. G., Hernick, M., and Fierke, C. A. (2010) *J Biol Chem* **285**, 33788-33796

CHAPTER III

CLONING AND FUNCTIONAL CHARACTERIZATION OF KDAC11

Introduction

There is considerable interest in the characterization of individual KDAC isoforms because pharmacological inhibition of KDACs has resulted in significant antitumor and anti-inflammatory activities in the mammalian cells. The 18 enzymes that make up the family of eukaryotic lysine deacetylases (KDACs) are divided into four classes based on sequence homology, cellular function, and localization. KDAC1, 2, 3, and 8 comprise class I and these isozymes are closely related to the yeast KDAC RDP3. Class II enzymes, which include KDAC 4,5,6,7,9 and 10 contain an extra domain that make them homologous to the yeast deacetylase KDAC1. The third class uses NAD as a cofactor to catalyze deacetylation and they are referred to as the Sirtuin deacetylases. KDAC11 is the sole member of class IV and this isozyme shares share 30 percent sequence homology with class I enzymes. In particular, the sequence of KDAC11 is similar to KDAC8(1-5).

KDAC11 has the shortest amino acid (aa) sequence (347 aa) among KDACs followed closely by KDAC8 (377 aa). Additionally, key residues that make up the active and substrate-binding sites are strictly conserved between these enzymes (Figure 1.3c)(6).

Finally, extensive studies on the known chromatin remodeling complexes have not identified KDAC11 and KDAC8 associated with known protein complexes in eukaryotic cells(7). This result suggests that these two isozymes may catalyze deacetylation of cellular targets other than histones. The exclusion of KDAC11 from the class I and II KDACs is based largely low sequence homology (30%) and the fact that KDAC11, which does not exist in fungi, is the only isozyme not present in all eukaryotic organisms.

Additionally, KDAC11 is express only in the brain, heart, skeletal muscle, kidney, and testis(8). Whereas class I KDACs are ubiquitously expressed in normal human tissues. Mammalian KDAC class I and II are grouped partly based on biochemical characterization and their biological role in the cell. For example, characterization of KDAC8 reveal common features seen in Class I. Several crystal structures of KDAC8 bound to inhibitors and substrates have revealed the bound divalent metal and *in vivo* studies suggest a specific role for KDAC8 in smooth muscle cells(9,10). KDAC6 displays Class II traits due to its deacetylation of the protein chaperone HSP90 in the cytoplasm as well as histone proteins in the nucleus(11). Despite poor biochemical characterization, there is growing evidence that indicate specific roles for KDAC11 in mammalian cells.

KDAC11 is proposed to play an important role in regulation of immune response. Antigen Presenting cells (APC) are responsible for the immune activation as well as immune tolerance. Pro- and anti-inflammatory cytokines greatly influence the functions of antigen presenting cells (APC). Specifically, the cytokine IL-12 is produced in response to an infection and the expression of the cytokine IL-10 restores immune tolerance upon the destruction of the antigen. Recently, studies have linked chromatin

accessibility to the expression of these cytokines. A recent study suggests that KDAC11 is a key player in determining immune activation vs. immune tolerance. Sotomayor colleagues demonstrated that KDAC11 interacts with the distal region of the promoter region of the interleukin 10 (IL-10) gene, an anti-inflammatory cytokine, and regulates its expression. During inflammation, expression of KDAC11 inhibits the expression of IL-10 causing the $CD4^{+}$-Tcell mediated expression of pro-inflammatory cytokines IL-12 and IL-1. Conversely, expression of IL-10 leads to adaptive immunity where IL-10 inhibits the CD4+ T cell mediated expression of IL-12 and IL1. Furthermore, aberrant expression of KDAC11 can result in a continued inhibition of IL-10 expression and continued activation of IL-12 expression leading to subsequent damage to regular cells. Therefore, these findings suggest that KDAC11 is a viable drug target for the treatment of autoimmune disease, organ rejection, and cancer. Additionally, the interaction of KDAC11 at the promoter of IL-10 suggests that KDAC11 could catalyze deacetylation of one of the histones or a transcription factor(12-14).

In addition to potentially catalyzing the deacetylation of histones, KDAC11 may recognize other protein substrates and regulate their function. Cdt1 is a DNA licensing replication factor that is required for the proper replication of DNA in mammalian cells. Regulation of Cdt1 is necessary to ensure that DNA is replicated only once per cell cycle. The concentration of Cdt1 increases in G_1 phase where it directly recruits the mini-chromosome maintenance (MCM) complex, a DNA helicase. Cdt1 is degraded in the S phase, which releases the MCM complex to sustain the cycle. Since active Cdt1 could catalyze a second round of MCM loading and therefore DNA replication, it is critical that Cdt1 is down-regulated or degraded at the start of S phase. Cdt1 activity is also inhibited

by Geminin, a 75 kDa protein that builds up in the S phase. Additionally, Cdt1 can be ubiquitinated and targeted for degradation by the proteasome and/or acetylated at the N-terminus suggesting that the function of this protein is regulated by acetylation and deacetylation. Seto and colleagues recently demonstrated that the two N-terminal lysines (Lys 24, Lys 34) of Cdt1 could be acetylated by lysine acetyl transferases 2B and 3B (KAT2B, KAT3B). Furthermore, transfection of cells with Myc-Cdt1 and FLAG-KDAC11 increases ubiquitinated Cdt1 by a factor of two. Therefore, one can envision a cellular mechanism where acetylation and ubiquitination are competitive. The KATs catalyze acetylation of Cdt1 in the G1 phase to prevent degradation, and KDAC11 catalyzes deacetylation of Cdt1 in the S-phase assuring that MCM loads onto DNA only once per cell cycle(15-19). These results are exciting since for the first time they describe a vital role for KDAC11 in regulating the function of a key protein involved in DNA replication.

Despite identification of important cellular functions of KDAC11, very little is known about its catalytic function. Sequence analysis demonstrates that KDAC11 retains all of the conserved residues that are crucial for efficient catalytic activity in class I and class II KDACs. Despite low sequence homology, KDAC11 contains the two conserved histidines (His142 and His143) in KDAC8 that are proposed to function as general acid/base and electrostatic catalysts. Furthermore, a Tyr (Tyr306 in KDAC8) that stabilizes the oxyanion intermediate catalysis is also conserved in KDAC11(20). The residues that coordinate the divalent metal (His180, Asp 183, Asp 267) are also conserved in KDAC11 (Figure 1.3a-c). These findings suggest that KDAC11 has deacetylase activity similar to KDAC8. However, the biochemical characterization of

KDAC11 is lacking due to the difficulty of assaying the catalytic activity of this enzyme *in vitro*.

One sequence alteration in KDAC11 compared to all the other KDACs is the Asp101 to Asn 101 substitution (Figure 1.3a-c). This side chain plays an important role in the molecular recognition of the widely used fluorescent substrates (Scheme 3.1) and inhibitors such as trichostatin A (TSA)(21). The crystal structure of KDAC8 TSA places this residue at the entrance of the active site near the substrate binding site. D101 makes two hydrogen bonds. The first is with the backbone NH group of the acetyl lysine residues and the second contacts the backbone NH group of the adjacent residue (n+1)(22). Decreased inhibition of KDAC11 by TSA and SAHA as well as low activity in catalyzing deacetylation of commercially available coumarin substrates could be attributed to the alteration of this side chain. Identifying substrate with enhanced reactivity would greatly aid in the enzymatic characterization of KDAC11 and the development of specific KDAC11 inhibitors.

Additionally, Class I and Class II KDACs are activated by divalent and monovalent cation. Divalent cations such as Fe^{2+} and Zn^{2+} play a central catalytic role by enhancing substrate affinity and neutralizing negative charge in the tetrahedral intermediate and the transition state and lowering the Pk_a of the metal-water nucleophile. Removal of divalent cations with chelating agent suppresses deacetylase activity demonstrating catalytic importance(23,24). KDAC activity also depends on the concentration of monovalent cations like K^+. KDAC8 activity is both activated and inhibited by monovalent cations. The crystal structure of KDAC8 visualized with two K^+ ions, one near (7 Å) and one distal (21 Å) from the catalytic metal. Mutagenesis studies

indicate that the inhibitory monovalent cation is located near the active site(25). Similarly, elevated K^+ concentration inhibits KDAC7(26). Therefore, it is plausible that these monovalent cations could regulate the activity of KDAC11.

This study reports on the cloning, purification, and biochemical characterization of KDAC11. We show that Fe^{2+} Co^{2+} and Zn^{2+} activate KDAC11. Mass spectrometric assay is used to analyze the reactivity of KDAC11 with a small library of peptides (GXK(ac)ZGC). This analysis demonstrates that KDAC11 has significant sequence preference and identifies a sequence motif recognized by KDAC11 *in vitro* and possibly *in vivo*. These data provide compelling evidence that KDAC11 is metal-dependent KDAC that has narrow substrate specificity.

Materials and Methods

Cloning of KDAC11

The human KDAC11 cDNA was purchase from Geneocopia in a plasmid that harbors an N-terminal His_6Sumo Tag (pB13x) (Genbank accession #: NP_07910). A silent mutation was introduced to remove an extra Xho1 site within the KDAC11 gene where the codon at Leu263 CTC was changed from CTC to CTA leaving a unique XhoI site at its C-terminus. The restriction endonucleases KpnI and XhoI (New England Biolabs) were used digest the pB13x plasmid and excise the KDAC11 gene between the SUMO tag and the C-terminal of KDAC11. Then, the KDAC11 gene was ligated into a Pet (pHD4) expression plasmid that presents a C-terminal Tobacco etch virus (TEV) cleavage site adjacent to a His_6 tag just upstream the stop codon. The KpnI site was engineered to a multiple cloning sites (MCS) located downstream of the T7 RNA polymerase promoter and ribosome binding site. The XhoI restriction site had previously been moved immediately N-terminal to the Tev-His_6 tag in the pHD4 plasmid. Following the digestion of the pHD4 vector with the restriction enzymes KpnI and XhoI, the KDAC11 fragment was ligated to pHD4 using T4 DNA ligase (New England Biolabs). The ligation plasmid (pHD4_KD11) was transformed into XL1-Blue Z-competent cells (Agilent Technologies) for colony screening and plasmid purification (QIAprep mini prep Kit, Qiagen). The KDAC11 gene was confirmed to be upstream of the Tev-His_6 tag by sequencing and digesting with Xho1 and Stu1 restriction enzymes. In this case, Stu1 cuts once within the KDAC11 gene.

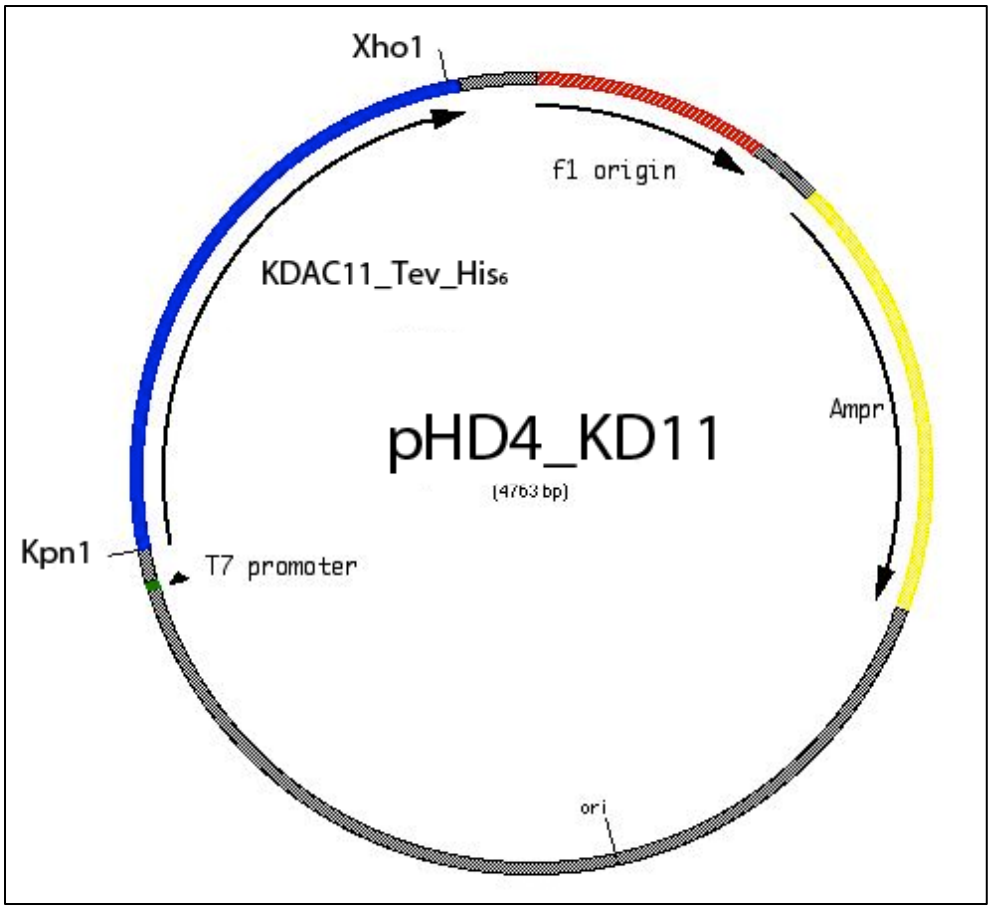

Figure 3.1. Plasmid map of KDAC11 *E. coli* expression vector

Purification of KDAC11

The pHD4_KD11 plasmid was transformed into the BL21 (DE3) strain of *E. Coli*. One ampicillin resistant colony was inoculated into 5 mL of 2XYT growth medium supplemented with ampicillin (5 µg/mL) and incubated at 37 ˚C for 6h. The culture was transferred to 2L of auto induction medium (TB growth medium, Novagen) that contains 10% glycerol and ampicillin (5 µg/mL) and incubated at 37 °C until OD 0.4-0.6. The temperature was then lowered to 20 °C for an additional 16 h incubation. In this medium, protein expression is induced in mid-log phase by the lactose as other carbons sources are depleted. The cells were harvested by centrifugation at 4000 rpm for 20 min, and resuspended in 30 mM Hepes / 80 mM NaCl /1mM tris(2-carboxyethyl)phosphine (TCEP) / 5% glycerol pH 8.0, lysed using a microfluidizer and the resulting extract was clarified by centrifugation at 15000 rpm for 40 min at 4 °C. The lysate was diluted 2-fold with Buffer A (30 mM HEPES, 1mM TCEP, 5% Glycerol, pH 8.0) and loaded onto a pre-packed anion exchange column (Hi-trap Q High Performance, GE Healthcare). The column was washed with 10-column volumes (cv) of Buffer B (BufferA + 150 mM NaCl) followed by a gradient elution from 150 mM to 300 mM NaCl. His_6Tag antibody was used confirm the expression of KDAC11. The fractions that contain KDAC11 were pooled and concentrated by centrifugation at 3500 rpm with Amicon Ultra-15 Centrifugal Filter Units to approximately 10 mL and reacted with Tev-protease (50:1) overnight at 4 °C. The protein was further fractionated on a size exclusion column (Sephacryl S-200 HR, GE Healthcare) in 25 mM MOPS pH 7.5, 250 mM NaCl, and 1 mM TCEP. The fractions that contained KDAC11 were pooled to yield >98% pure protein.

Apo-KDAC11

Apo KDAC11 was prepared by dialyzing the purified enzyme twice for 12h against 25 mM 4-morpholinepropanesulfonic acid (MOPS), 1 mM EDTA, and 10 μM dipicolinic acid (DPA), pH 7.5, followed by dialysis against 25 mM MOPS, and 1 μM EDTA, pH 8.0. The enzyme was then concentrated using an Amicon Ultra Microcon centrifugal filtration device (10,000 MWCO) and the buffer was exchanged using a PD-10 gel filtration column (GE Healthcare) equilibrated with 25 mM MOPS, pH 8.0 (pretreated with metal chelating resin, Chelex 100). The metal content of the protein was determined by inductively coupled plasma emission mass spectroscopy (ICP-MS) (Department of Geological Sciences, University of Michigan). The final concentration of KDAC11 was determined by both OD_{280} (ε_{280} =42523 $M^{-1}cm^{-1}$, under denaturing conditions) and the absorbance change after reaction with 5,5'-dithiobis(2-nitrobenzoic acid) (ε_{412} =13,600 $M^{-1}cm^{-1}$).

Western blot analysis

KDAC11 expression was confirmed using a C-terminal His_6 antibody. Following the anion exchange, separation 10 μl of pooled fractions (chosen after inspection of SDS PAGE gel) that contain KDAC11 was electrophoresed on a 12% SDS PAGE gel (BioRad), transferred to a nitrocellulose membrane, and immunoblotted using the anti-mouse monoclonal antibody (1:1000) for C-terminal His_6 (invitrogen). The alkaline phosphatase (AP) labeled primary anti-body was detected using detected using an AP Detection Reagent Kit (novagen).

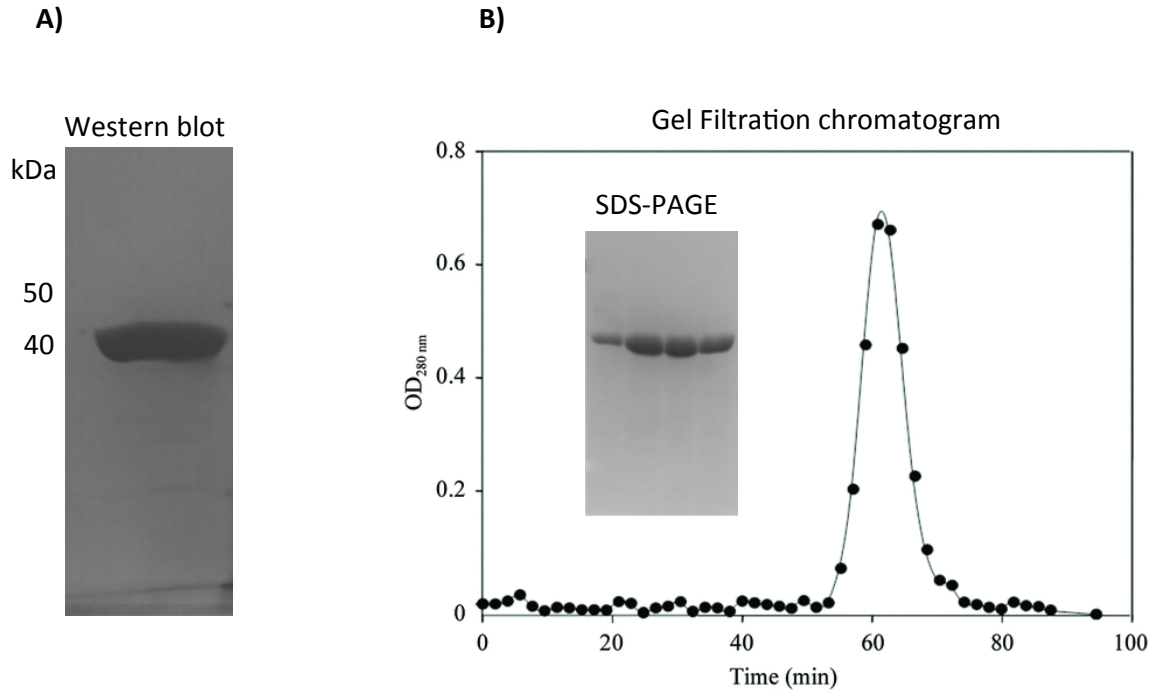

Figure 3.2. Purification of KDAC11. A) Detection of anti-C-terminal His_6. B) Gel filtration chromatogram and SDS PAGE gel of fractions from the gel filtration peak.

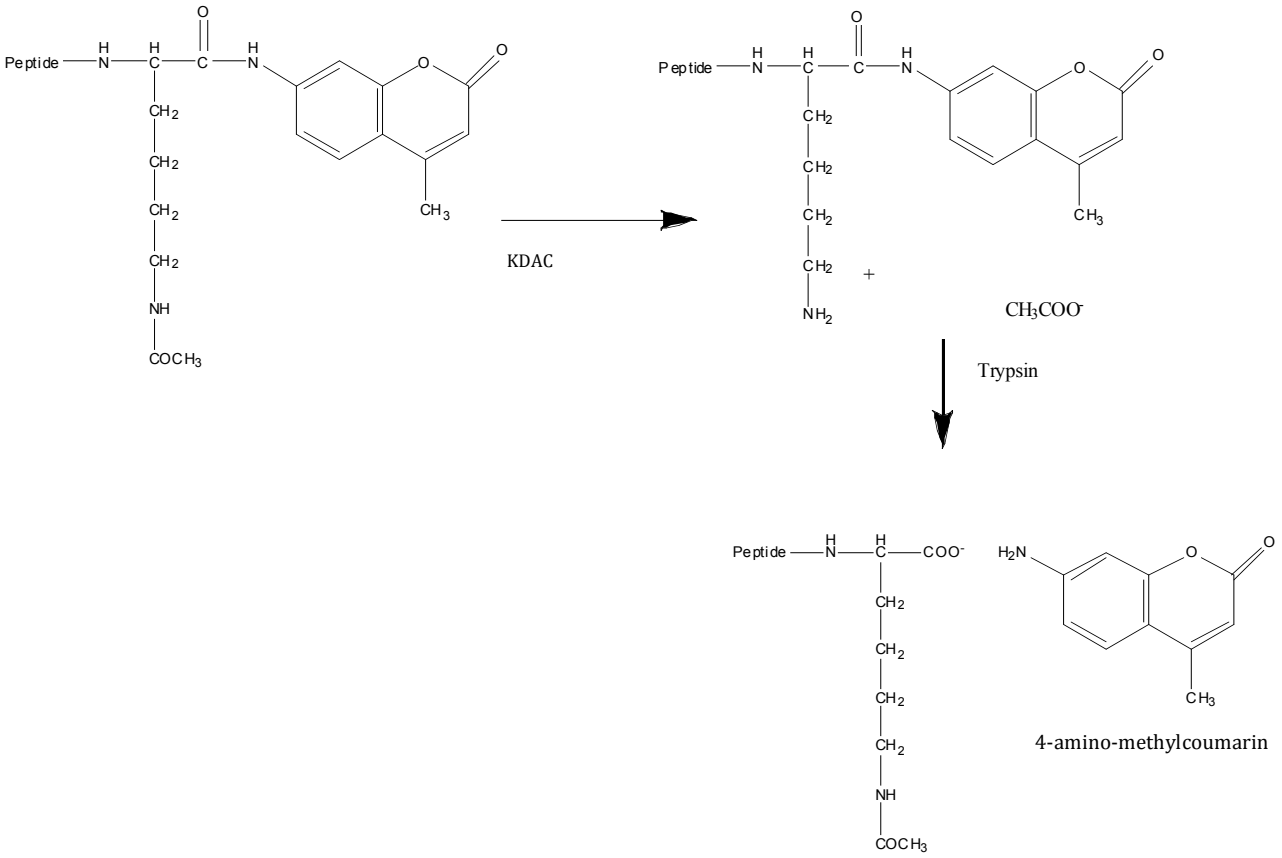

Scheme 3.1. Fluor-de-Lys KDAC assay.

Fluor-De-Lys Assay

The catalytic activity of wild-type KDAC11 was measured using a commercially available fluorescent assay (Enzo Life Sciences) with the Fluor-de-Lys P53 substrate. The substrates contain ε-acetylated lysine residue followed by C-terminal 4-methylcoumarin-7-amide (MCA). Cleavage of the C-terminal lysine of the substrate by HDAC allows proteolysis catalyzed by trypsin, resulting in a shift in the wavelength and intensity of the fluorescence of the MCA moiety (Scheme 3.1). Trichostatin A (10 μM TSA), a potent HDAC inhibitor, was used to quench the reaction. All assay buffers were pre-treated with Chelex resin (Bio-Rad) to remove trace divalent metal ions. Metal-free KDAC11 was reconstituted with Co^{2+}, Zn^{2+} and Fe^{2+} by incubation with equimolar concentrations of metals in assay buffer (25 mM Tris pH 8.0, 137 mM NaCl) pretreated with Chelex resin (BioRad). All Fe^{2+} assays were performed in an anaerobic chamber (Coy laboratories). Fluorescence was monitored at λ_{ex} = 340 and λ_{em} = 450 for the deacetylated and cleaved product, and at λ_{ex} = 340 and λ_{em} = 380 for the acetylated substrate. The amount of product formed was determined from a standard curve made up of known concentrations of products and substrates. The steady-state kinetic parameter k_{cat}/K_m was determined from initial reaction rates using 1 μM M^{2+}-KDAC11 and 50 μM substrate in assay buffer at 25 °C.

Mass Spectrometry

Peptide library studies were performed using an assay where 384 acetylated peptides were immobilized on alkenothiolate monolayer that presents a maleimide group. Matrix-assisted laser desorption ionization time-of-flight mass spectrometry (MALDI TOF MS) spectra are taken of the immobilized peptide substrate before and after treatment with KDAC11 (Figure 2.1). To form the immobilized peptide library, 3 μL of the cysteine-terminated peptides were transferred to each well to react with the maleimide moeity at 37˚C for 1 h. KDAC11 was reconstituted with either Zn^{2+}, Fe^{2+}, and Co^{2+}, in the assay buffer (25 mM MOPS, 80 mM NaCl, pH 7.5) and incubated on ice for 30 min. The plates were washed with ethanol/water/ethanol followed by reaction with KDAC11 (1 μM) at 30 ˚C for 30 min. KDAC11 was stopped with additional ethanol/water/ethanol rinses and the plates were dried under nitrogen gas. A matrix (2,4,6-trihydroxyacetophenone, 25 mg/mL in acetone) was applied to each plate and air-dried. The plate was loaded on the 4800 MALDI mass spectrometer (Applied Biosystems) and a spectrum was obtained.

Acetate assay

An assay that couples the formation of the product acetate to an increase in NADH, as measured by fluorescence (Scheme 2.1), was used to measure the steady-state kinetic parameters for catalytic deacetylation of peptides without the MCA fluorophore. This assay couples three enzymatic reactions. The first enzyme catalyzes the reaction of acetate with adenosine-5'-triphosphate (ATP) and Coenzyme A (CoA) to form Acetyl-CoA ADP and P_i. In the second step, Acetyl-CoA reacts with oxaloacetate, catalyzed by

citrate synthase, to produce citrate and CoA. Oxaloacetate is produced from the reaction of malate and NAD to form oxaloacetate and NADH, catalysed by malate dehydrogenase Thus, the consumption of oxaloacetate by the reaction with AcCoA produces an increase in NADH concentration which is monitored at λ_{ex} = 340 nm and λ_{em} = 460 nm. Steady-state kinetic parameters were determined from initial rate reactions (10 µL total) containing 0.2 µM KDAC11 apo or metal bound, and varying peptides concentrations (5-400 µM). Apo KDAC11 was incubated with equimolar concentration of Fe^{2+}, Zn^{2+} and Co^{2+} in 25 mM MOPS 80 mM NaCl, pH7.5 for 30 min prior to initiating the reaction with peptides. The reactions were stopped by addition of 0.1% HCl and neutralized with 1% sodium bicarbonate to a final volume to 10 µL prior to detection of acetate using the coupled assay. For acetate detection, the enzymes and substrates were purchased from R-Biopharma and mixed according to the instructions. 8µl of neutralized solution deacetylase reaction was added to 60 µL of coupled enzyme reaction mixture for 30 min prior to loading onto a 96 well plate (Half Area Black Flat Bottom Polystyrene non-binding surface, Corning) and measurement of the fluorescence read on a plate reader (BMG Latech, FLUOstar Galaxy). Amount of product was determined from a standard curve calculated using a known concentration of acetate.

RESULTS

Cloning and purification of KDAC11

Sequence alignment and secondary structure prediction of KDAC11 and KDAC8 shows conservation of the deacetylase domain (Figure 1.3c). The general acid/general base and electrostatic catalyst residues H142 and H143 are conserved and Tyr306, proposed stabilize the transition state, is also conserved. The key difference between the two sequences is Asp101, which is replaced with an uncharged Gln101 in KDAC11. The loops (L1-L7) seen in KDAC8 appear to be retained in KDAC11. The metal-binding site residues are conserved and appear to be in similar secondary structure fold as KDAC8. The side chains in loop 3 and 7 that line the active site in KDAC8 do the same in KDAC11. These results suggest that KDAC11 possesses the common structural and mechanistic features that are important for deacetylase activity.

To examine the catalytic property of KDAC11, I recombinantly expressed the protein in *E. coli*. The commercially available expressin vector of KDAC11 (pB13x, Geneocopia) with a N-terminal His_6Sumo yielded 1 mg of KDAC11 per liter of *E. coli* after induction with 0.5 mM Isopropyl-β-D-thio-galactoside in 2xYT medium. The poor yield was due to low expression and poor binding of the His_6Sumo tag to the Ni^{2+}-charged IMAC column. The His_6 antibody detected the His_6 tag in the flow-through and wash steps of the IMAC column, confirming the poor binding. To increase the yield of KDAC11, KDAC11 gene was subcloned onto a new pET-derived expression plasmid with a C-terminal Tev-His_6 tag (Figure 3.1). This plasmid was transformed in *E. coli.* BL21 (DE3) and expression of KDAC11 was induced using auto-induction (TB)

medium. A new purification method was developed combining an anion exchange and gel filtration chromatography, rather than using the His tag Ni^{2+} affinity resin. This strategy yields 6-7 mg of > 98% pure KDAC11 per liter of auto-induction (TB) medium.

Reactivity of KDAC11

Next, we measured the steady state kinetics of the deacetylation of the commercially available coumarin substrate catalyzed by KDAC11. Before assaying, metal ions were removed by incubation with chelators; ICP-MS analysis confirmed the presence of ≤ 0.01 $mole^{Metal/}mole^{KDAC11}$. KDAC11 was reconstituted with metal by addition of an equimolar concentration of Zn^{2+}, Co^{2+} and Fe^{2+} and incubation on ice for 30 min. Following reconstitution, Fluor-de-Lys (FDL) assay was performed to measure the reactivity of apo, Zn^{2+} $Fe^{2+}$and Co^{2+}-bound KDAC11 for catalyzing deacetylation of the coumarin substrate (50μM) using 1μM KDAC11 (Scheme 3.1). The value for k_{cat}/K_m for deacetylation was measured as: 966 ± 76 $M^{-1}s^{-1}$ (Co^{2+}), 100 ± 16 $M^{-1}s^{-1}$ (Zn^{2+}), and < 1 $M^{-1}s^{-1}$ (Fe^{2+} and apo-KDAC11). These data demonstrate that the deacetylase activity of KDAC11 is activated by divalent cations. However, The Co^{2+}-KDAC11 k_{cat}/K_m is 10-fold lower that that of KDAC8 (10, 000 $M^{-1}s^{-1}$) under the same conditions.

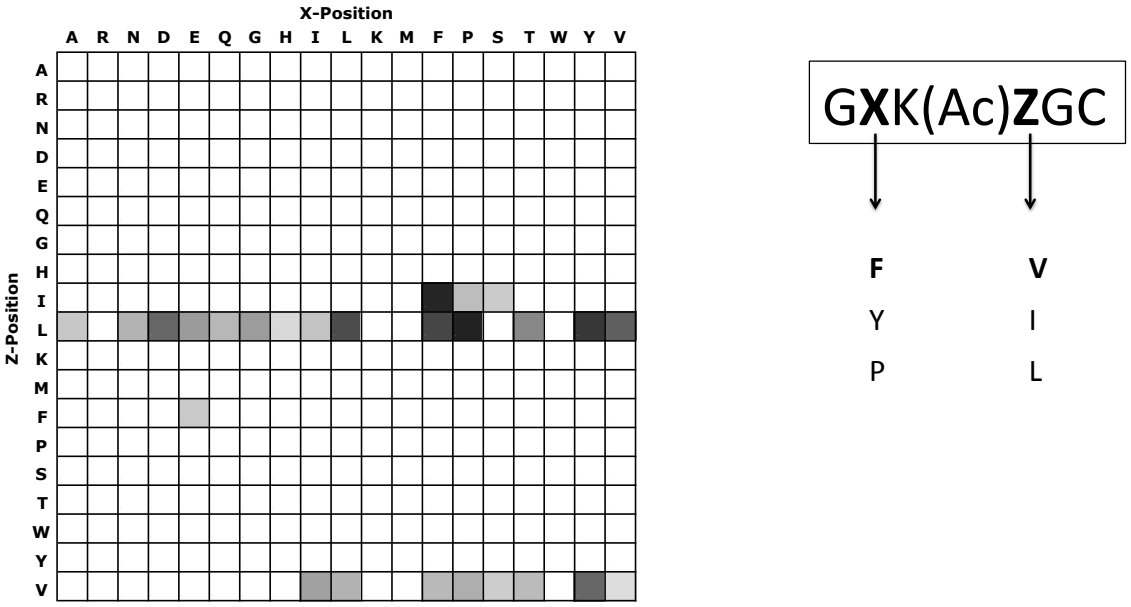

Figure 3.3. Substrate Selectivity of Co^{2+}-bound KDAC11. Assays were performed with MALDI TOF MS. G**X**K(Ac)**Z**GC peptide library (X and Z represent all AAs except Cys). 1 μM KDAC11. Buffer: 25 mM MOPS pH8, 80 mM NaCl, 30 °C for 1 h. Arrows indicate sequence preference.

Substrate selectivity of KDAC11

Peptide libraries have been widely used to identify sequence motifs recognized by post-translational modifying enzymes(27,28). To identify sequence motifs recognized by KDAC11, we assayed the reactivity with a library of peptides. This library was composed of 384 peptide substrates (GXK(ac)ZGC) that were immobilized on MALDI plate by reacting a maleimide group with the cysteine residue located two residues downstream of the acetylated lysine (n+2). Following immobilization of the substrates on the plate, 1 μM of Zn^{2+} Fe^{2+}or Co^{2}-bound KDAC11 was added to the plate and incubated for 30 min at 37 ˚C (Figure 2.1). After stopping the reaction by washing with ethanol/water/ethanol, a MALDI spectrum was obtained for each plate. No deacetylation was observed for incubation with Apo, Zn^{2+} Fe^{2+}-bound KDAC11. The Co^{2+}-bound enzyme catalyzed the deacetylation of the 32 out 384 peptides with the highest reactivity with KDAC11 having a hydrophobic residues at both X(such a Phe, Pro, or Tyr) and Z (Leu) positions.. The highest deacetylase activity was seen in the following peptides (GFK(Ac)LGC, GPK(Ac)LGC, GYK(Ac)LGC) were 15, 18 , 23 % deacetylation respectively. Based on this specificity, we searched the literature to identify acetylated potential proteins that substrates for KDAC11(6,12,29). Sequence analysis of three protein candidates, histones H3 and H4 and DNA replication licensing factors, reveal that the sequence of an acetylated lysine residue located on the N-terminal of Cdt1 is a close match.

Steady state kinetic analysis of KDAC11

To further examine the substrate selectivity of KDAC11, peptides sequences corresponding to the sequence motif in Cdt1 (IIAPPKLAC) was synthesized and assayed. The steady state kinetic parameters for deacetylation catalyzed by KDAC11 were measured by monitoring the increase in the concentration of the acetate product using a coupled assay measured an increase in NADH. The k_{cat}/K_m ($\mu M^{-1}s^{-1}$) values for Fe^{2+}, Zn^{2+}, and Co^{2+}-bound KDAC11 on the IIAPPKLAC peptide sequence are 0.65 ± 0.3, 0.33 ± 0.04, and 0.47 ± 0.08 respectively. Remarkably, the k_{cat}/K_m value for Co^{2+}-KDAC11 is increased 650-fold compared to the coumarin substrate (Table 3.1). Furthermore, the shorter peptide (GPK(ac)LAC) is even a better substrate for KDAC11 with values of k_{cat}/K_m approaching $5x10^5$ (Table 3.1). The error on k_{cat}/K_m on this peptide is large as k_{cat}/K_m value approaches the limit of detection of the assay (1μM, Table 3.1). These results validate the peptide sequence IIAPPKLAC as a efficient substrate for KDAC11 and demonstrate that KDAC11 requires only a short sequence for efficient substrate recognition. Furthermore, for the more specific substrates, comparable activity is observed for the enzyme substituted with Co^{2+}, Fe^{2+}, and Zn^{2+}, suggesting the possibility that a variety of metal cofactors could activate KDAC11 *in vivo*.

	IIAPPKLAC			PK(ac)LAC		
M^{2+}	k_{cat}/K_m ($\mu M^{-1}S^{-1}$)	k_{cat} (S-1)	K_m (μM)	k_{cat}/K_m ($\mu M^{-1}S^{-1}$)	k_{cat} (S-1)	K_m (μM)
Zn^{2+}	0.33 ± 0.04	3.6 ± 0.02	10.7 ± 3.2	0.74 ± 0.44	2.42 ± 0.22	3.25 ± 2.10
Co^{2+}	0.47 ± 0.08	2.55 ± 0.09	5.5 ± 1.1	2.37 ± 1.26	3.55 ± 0.22	2.37 ± 1.26
Fe^{2+}	0.65 ± 0.31	2.34 ± 0.04	4.5 ± 5	4.5 ± 2.54	5.23 ± 0.23	1.16 ± 0.68

Table 3.1. Steady state kinetic parameters of metal-bound KDAC11.

Discussion

In this study, we describe the expression and functional characterization of the newest member of the KDAC family. KDAC11 is the only member of the class IV deacetylases and the smallest member of the 18 KDACs identified. It has distinct expression patterns and is the only isoform not observed in Fungi. Due to conservation of the deacetylase domain KDAC11 was proposed to have deacetylase activity although no data was available to support it. Interestingly, here we demonstrate this activity *in vitro*. Activity assays using the fluorescently-labeled coumarin substrate demonstrate KDAC11 deacetylase activity in *E.coli* cell lysates(14). However, consistent with the findings of other labs, the activity of the recombinant KDACs was not observable during purification. Therefore, we initially used PAGE analysis and western blots to follow the fractionation of KDAC11. To obtain active recombinant KDAC11, we reconstituted the enzyme with stoichiometric metal, altered the assay conditions, and varied the sequence of the peptide substrate as described in detail below.

Many zinc metalloenzymes are both activated by stoichiometric metal ions and inhibited by additional bound metal ions. Upon cell lysis, the free concentration of the metal ions, such as Zn^{2+}, may increase significantly due to oxidation of thiol ligands. Additionally, enzymes activated by redox-sensitive metal ion, such as Fe^{2+}, may lose activity after lysis due to metal oxidation(30). To examine whether the loss of KDAC11 activity was related to the active site metal ion, we removed all bound metals using a chelator and then reconstituted with stoichiometric of Fe^{2+}, Zn^{2+}, and Co^{2+}. The reconstitution of Co^{2+} significantly enhanced the reactivity of KDAC11 with the coumarin peptide substrate. Decreased activity was observed for the Zn^{2+}-KDAC11 and

little activity for the Fe^{2+}-KDAC11. Therefore, metal reconstitution was important for observing the activity of recombinant KDAC11. However, Co^{2+} is not likely to the *in vivo* cofactor.

Furthermore, the KDAC buffers sold with the FDL kit contain 147 mM NaCl, and 10 mM KCl, which is optimal for the activity of KDAC8. KDAC8 is both activated and inhibited by monovalent cations and K^+ is particularly inhibitory at high concentrations. To examine whether KCL inhibits KDAC11 at low concentrations, we measured the activity in buffer containing only 80 mM NaCl. Experiments to further define the monovalent-dependence of KDAC11 are currently underway. Alteration in the monovalent cation dependence may be important for the *in vivo* function.

We also examined the peptide selectivity of KDAC11. A dearth of commercially-available peptide substrates are available for characterization of the *in vitro* activity of KDACs. The widely used coumarin substrate is limited by the location of the coumarin fluorophore next to the acetylated lysine. To identify sequence motifs recognized by KDAC11, we used a mass spectrometric assay to screen the reactivity of KDAC11 with a peptide library. Since we observed that KDAC11 activity alters with the bound metal ion, we measured the reactivity of the peptide library with Co^{2+}, Zn^{2+}, and Fe^{2+}-bound KDAC11 using apo-KDAC11 as a control. Interestingly, unlike KDAC8, KDAC2 and KDAC3 whose profiles show broad substrate reactivity(27,28), Co^{2+}-KDAC11 has specific sequence preferences with increased reactivity for hydrophobic groups flanking both sides of the acetylated lysine (Figure 3.3).

Knockout of specific KDAC isozyme although generally lethal, does not necessarily result in an increase of a targeted substrate(31). However, knockout of

KDAC11 directly correlates with the increase of pro-inflammatory cytokine IL-10 that leads to immune tolerance. Additionally, the negatively charged side chain of Asp101 is seen in the crystal structure of KDAC8 making hydrogen bond with amide nitrogen of the acetylated lysine and a Asn101 in KDAC11 replaces this residue. This residue is implicated in the broad substrate specificity of KDAC8 and most KDACs. Broad substrate selectivity is a crucial property in the KDAC family due to the large number of acetylated substrates found in mammalian cells.

These results indicate that KDAC11 is more selective for the peptide sequence compared to other KDAC isozymes. No deacetylase activity was observed for the Zn^{2+}-bound or the Fe^{2+}-bound KDAC11 on the peptide arrays. It is possible that metal contaminations on the surface of the peptide array inhibit the KDAC11 activity. The specific substrate profile seen with the Co^{2+}-bound KDAC11 provided information crucial to identifying sequence motifs recognized by KDAC11.

To follow up on the peptide library studies, we searched for sequences in proteins proposed to associate with KDAC11 that match the sequence motif identified by the peptide library. Histone proteins (H3 and H4) and Cdt1 have been proposed to interact with KDAC11 based on transfection and Chromatin immunoprecipitation (ChIP) methods. Excitingly, a sequence near the N-terminus of Cdt1, a protein that plays a critical role in the licensing of DNA for replication closely resembles the KDAC11 optimal substrate (Table 3.1). Several reports have shown that Lys 24 on Cdt1 is acetylated by KATs 3B and 2A(15). Previous studies have demonstrated that KDAC11 associates with Cdt1 and regulates its function(29); however, previous data have demonstrated that this regulation occurs through deacetylation of Lys 24. To investigate

the catalytic efficiency of KDAC11 on this sequence we used an assay that coupled the release of acetate to the increase in the concentration of NADH, monitored fluorescently. Excitingly, the k_{cat}/K_m value for this substrate is high, 3-6 x 10^5 $M^{-1}s^{-}1$. The Fe^{2+}-bound KDAC11 decreases the Km value for this substrate. The catalytic efficiency for the shorter sequence GPK(ac)LAC is even higher suggesting that KDAC11 recognizes short sequence motifs. The crystal structure of KDAC8 indicates that only 6 residues interact with this enzyme. Hence, KDAC11 could similarly recognize short peptides. Reactivity of the Fe^{2+}-KDAC11 activity is modestly higher for both sequences compare to the Zn^{2+}-KDAC11 suggesting the either divalent ion is the metal ion that activates KDAC11 *in vivo*. Furthermore, these sequences are great substrates for assay the activity of KDAC11 in vitro. Finally, the correlation of this sequence and sequence observed in KDAC11 associated proteins suggest that this is also a sequence recognition motif in *in vivo* substrates

In summary, we describe the cloned characterized catalytic properties of KDAC11. Using a peptide library we identified a sequence motif recognized by KDAC11 *in vitro* and possibly *in vivo*. Also, we showed that KDAC11 activity is activated by metal ion that is essential for activity. These data suggest that KDAC11 activity is also be regulated by monovalent cations, as observed in KDAC8. Finally, KDAC11 has a narrow substrate selectivity compared other KDAC isozymes suggesting a more specific role for the function of KDAC11, consistent with the limited *in vivo* expression KDAC11.

BIBLIOGRAPHY

1. Grozinger, C. M., Hassig, C. A., and Schreiber, S. L. (1999) *Proceedings of the National Academy of Sciences of the United States of America* **96**, 4868-4873

2. Keedy, K. S., Archin, N. M., Gates, A. T., Espeseth, A., Hazuda, D. J., and Margolis, D. M. (2009) *Journal of virology* **83**, 4749-4756

3. Lahm, A., Paolini, C., Pallaoro, M., Nardi, M. C., Jones, P., Neddermann, P., Sambucini, S., Bottomley, M. J., Lo Surdo, P., Carfí, A., Koch, U., De Francesco, R., Steinkühler, C., and Gallinari, P. (2007) *Proceedings of the National Academy of Sciences of the United States of America* **104**, 17335-17340

4. Lane, A. A., and Chabner, B. A. (2009) *Journal of clinical oncology : official journal of the American Society of Clinical Oncology* **27**, 5459-5468

5. Johnstone, R. W. (2002) *Nature reviews. Drug discovery* **1**, 287-299

6. Gao, L., Cueto, M. A., Asselbergs, F., and Atadja, P. (2002) *The Journal of biological chemistry* **277**, 25748-25755

7. Liu, H., Hu, Q., Kaufman, A., D'ercole, A. J., and Ye, P. (2008) *J Neurosci Res* **86**, 537-543

8. De Ruijter, A. J. M., Van Gennip, A. H., Caron, H. N., Kemp, S., and Van Kuilenburg, A. B. P. (2003) *Biochem J* **370**, 737-749

9. Dowling, D. P., Gattis, S. G., Fierke, C. A., and Christianson, D. W. (2010) *Biochemistry* **49**, 5048-5056

10. de Leval, L., Waltregny, D., Boniver, J., Young, R. H., Castronovo, V., and Oliva, E. (2006) *Am J Surg Pathol* **30**, 319-327

11. Kekatpure, V. D., Dannenberg, A. J., and Subbaramaiah, K. (2009) *The Journal of biological chemistry* **284**, 7436-7445

12. Georgopoulos, K. (2009) *Nature immunology* **10**, 13-14

13. Lai, X., Li, J. Z., Lian, Z. R., Niu, B. L., Chen, Y., Liao, W. Y., Liu, Z. J., and Gong, J. P. (2011) *Transplantation proceedings* **43**, 2728-2732

14. Villagra, A., Cheng, F., Wang, H.-W., Suarez, I., Glozak, M., Maurin, M., Nguyen, D., Wright, K. L., Atadja, P. W., Bhalla, K., Pinilla-Ibarz, J., Seto, E., and Sotomayor, E. M. (2009) *Nature immunology* **10**, 92-100

15. Glozak, M. A., and Seto, E. (2009) *The Journal of biological chemistry* **284**, 11446-11453

16. Buglio, D., Khaskhely, N. M., Voo, K. S., Martinez-Valdez, H., Liu, Y.-J., and Younes, A. (2011) *Blood* **117**, 2910-2917

17. Miotto, B. (2011) *Cell cycle (Georgetown, Tex.)* **10**, 1522

18. Wang, H., Cheng, F., Woan, K., Sahakian, E., Merino, O., Rock-Klotz, J., Vicente-Suarez, I., Pinilla-Ibarz, J., Wright, K. L., Seto, E., Bhalla, K., Villagra, A., and Sotomayor, E. M. (2011) *Journal of immunology (Baltimore, Md. : 1950)* **186**, 3986-3996

19. Wohlschlegel, J. A., Dwyer, B. T., Dhar, S. K., Cvetic, C., Walter, J. C., and Dutta, A. (2000) *Science (New York, N.Y.)* **290**, 2309-2312

20. Wu, R. B., Wang, S. L., Zhou, N. J., Cao, Z. X., and Zhang, Y. K. (2010) *Journal of the American Chemical Society* **132**, 9471-9479

21. Lombardi, P. M., Cole, K. E., Dowling, D. P., and Christianson, D. W. (2011) *Curr Opin Struct Biol* **21**, 735-743

22. Vannini, A., Volpari, C., Gallinari, P., Jones, P., Mattu, M., Carfí, A., De Francesco, R., Steinkühler, C., and Di Marco, S. (2007) *EMBO reports* **8**, 879-884

23. Hernick, M., and Fierke, C. A. (2005) *Arch Biochem Biophys* **433**, 71-84

24. Gantt, S. L. (2006) Human Histone Deacetylase 8: Metal Dependence and Catalytic Mechanism. in *Biologican Chemistry*, University of Michigan, Ann Arbor, MI

25. Gantt, S. L., Joseph, C. G., and Fierke, C. A. (2010) *J Biol Chem* **285**, 6036-6043

26. Schuetz, A., Min, J., Allali-Hassani, A., Schapira, M., Shuen, M., Loppnau, P., Mazitschek, R., Kwiatkowski, N. P., Lewis, T. A., Maglathin, R. L., McLean, T. H., Bochkarev, A., Plotnikov, A. N., Vedadi, M., and Arrowsmith, C. H. (2008) *The Journal of biological chemistry* **283**, 11355-11363

27. Gurard-Levin, Z. A., Kilian, K. A., Kim, J., Bahr, K., and Mrksich, M. (2010) *ACS Chem Biol* **5**, 863-873

28. Gurard-Levin, Z. A., Kim, J., and Mrksich, M. (2009) *Chembiochem : a European journal of chemical biology* **10**, 2159-2161

29. Wong, P. G., Glozak, M. A., Cao, T. V., Vaziri, C., Seto, E., and Alexandrow, M. (2010) *Cell cycle (Georgetown, Tex.)* **9**, 4351-4363

30. Maret, W. (2011) *Biometals : an international journal on the role of metal ions in biology, biochemistry, and medicine* **24**, 411-418

31. Haberland, M., Montgomery, R. L., and Olson, E. N. (2009) *Nat Rev Genet* **10**, 32-42

CHAPTER IV[1]

FUNCTION OF ARG37 IN THE INTERNAL CAVITY OF KDAC8

Introduction

One of the major hurdles in the development of KDAC inhibitors (KDACi) is achieving iso-form/class selectivity. Selectivity is hindered by the homologous nature of the deacetylase domain of the KDAC isozymes, which includes the active site residues, an 11 Å channel that accommodates the acetylated lysine of the substrate, and the residues that coordinate the catalytic metal ion(1-4). Mimicking these structural elements, KDACi share a common pharmacophore that is composed of a capping group that interacts the rim of the 11 Å channel, a region that fits into the channel leading to the active site and a metal binding moiety. Suberoylanilide hydroxamic acid (SAHA) and Romedopsin are the only FDA-approved KDACi (Table 1.1). However these are both broad-spectrum inhibitors that recognize both class I and class II KDACs *in vivo*(5-7). Given that there are over 3000 acetylated proteins and only 18 KDACs in mammalian cells, is it expected that KDACs would catalyze deacetylation on substrates that are both

[1] This work was published in collaboration with Matthew Fuchtner at Imperial College in London

specific for a single isozyme and recognized by multiple isozymes. KDACs exhibit distinct expression pattern and cellular localization, and unchecked activity of a specific KDAC can be related to the pathogenesis of a particular disease. However, limited selectivity of current KDACi leads to broad biological activities and difficulty in targeting a disease phenotype to a specific KDAC isozyme(8-10). Therefore, a goal is to develop isoform-specific KDACi that can enhance the treatment of specific diseases.

In addition to the therapeutic benefits of isoform/class-specific KDACi, these inhibitors may help distinguish the functions of each KDAC isozyme. It is intriguing that KDACi predate the discovery of KDACs. Trapoxin, a cyclic depsipeptide inhibitor, was used as an affinity tag to purify the first identified KDAC, KDAC1(11). Structure-activity relationships with selective inhibitors can also help interactions important for the molecular recognition by KDACs. Isoform-specific inhibitors can also facilitate high-resolution structural studies of KDACs. Finally, isoform- specific inhibitors can be labeled with a fluorophore for use in the discovery of new inhibitors and for the analysis of the location of isozymes in cells. Therefore, isoform-specific KDACi can help probe the structural and chemical basis for KDAC functions.

In the crystal structures of histone deacetylase-like protein (HDLP) complexed with trichostatin A (TSA) and KDAC8 complexed with TSA, the inhibitor binds in the hydrophobic 11 Å tube-like substrate channel that leads to the active site. In addition, a second 14 Å internal cavity lies adjacent to the metal active site and is lined by charged residues on one side and hydrophobic side chains on the other. Computational studies on the role of this internal cavity in HDLP suggest that acetate dissociate form this enzyme via this second channel(2,12,13). Consistent with this hypothesis, one of the crystal

structures of KDAC8 shows that the internal cavity is exposed to the outside environment, seemingly indicating flexibility in the opening and closing of this channel. Inspection of the X-ray crystal structure of KDAC8 revealed a conserved Arg37 residue at the center of this channel. Arg37 forms multiple hydrogen bonding interactions with the backbone carbonyl oxygen atoms of conserved glycine residues (Gly303 and Gly305) positioned in a loop between the β8 sheet and the α10-helix (Figure 4.1). These interactions tether the loop in position where the backbone amide of G303 forms a hydrogen bond with the carbonyl oxygen of the conserved Gly139 located in the loop between the β3 sheets and the α6-helix. The residues surrounding the 14 Å cavity are less conserved compare to residues that line the active site and substrate binding site so it is possible that this cavity may be exploited for designing isoform-specific inhibitors. Here, we probe the functional role Arg37 in this cavity, demonstrating that this side chain stabilizes both the acetate affinity and the transition state for deacetylation. Therefore, this residue is important efficient deacetylation catalyzed by KDAC8.

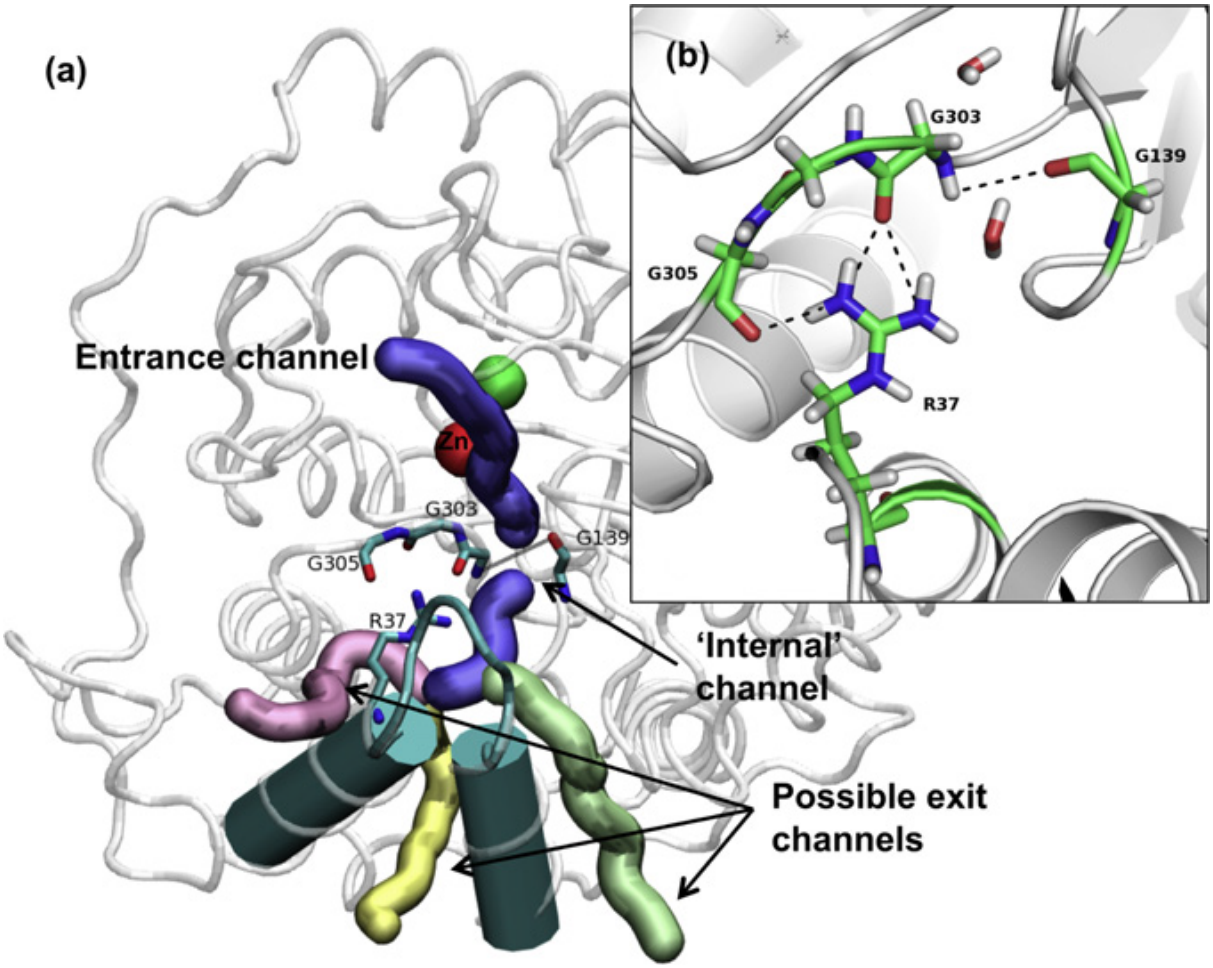

Figure 4.1[2]. Structure of KDAC8 showing Arg37 interactions. A) KDAC8 Structure showing interactions in the 14 Å channel of residues R37, G139, G303 and G305 depicted. (b) Tethering of the loop between β8 and α10-helix by R37.

[2] Figure 4.1 was made by Matthew Fuchtner

Materials and Methods.

Expression and Purification

The sequence for the KDAC8 gene was subcloned behind a T7 RNA polymerase promoter in a pET-20b derived expression plasmid with a C-terminus TEV-His tag (pHD4). KDAC8 mutants were constructed using the Quickchange Mutagenesis Kit (Strategene). After transforming the plasmid into the BL21(DE3) strain of E. coli, one colony was inoculated into 5 mL 2X-YT starter culture supplemented 0.1 mg/ml ampicillin and incubated for 4 h at 37°C . The starter culture was used to inoculate 6 L of 2X-YT media supplemented with 0.1 mg/ml ampicillin and incubated at 37°C until OD_{600} = 0.6-0.7, and then the temperature was reduced to 25 °C for 45 min. Protein synthesis was induced by the addition of 0.5 mM isopropyl β-D-1-thiogalactopyranoside (IPTG) and the cells were incubated for an additional 12-15 hours at 25 °C. The cells were harvested by centrifugation, resuspended in buffer A (30 mM Hepes, 150 mM NaCl, 0.5 mM imidazole, pH 8.0), lysed using a microfluidizer and the resulting extract was clarified by centrifugation (15000 rpm, 40 min, 4 °C). The cell extract was loaded onto a 10 mL metal affinity (GE Healthcare, Chelatin Fast Flow Sepharose) resin column charged with 150 mM nickel chloride. The column was washed with Buffer A containing 25 mM imidazole and then the protein was eluted with Buffer A containing 250 mM imidazole. The His_6-TEV tag was removed by incubation with recombinant TEV protease (100:1, protease: fusion protein) at 4°C and KDAC8/TEV protease then dialyzed overnight in buffer A containing 1 mM tris(2-carboxyethyl) phosphine (TCEP). The nickel column was ran a second time and the cleaved KDAC8 was obtained in the flow

through. 1-2 mg of > 98% pure KDAC8 was obtained per liter of 2 XYT medium using this protocol.

Apo WT and mutant KDAC8

Metal-free KDAC8 was prepared by dialyzing the purified enzyme twice overnight against 25 mM 4-morpholinepropanesulfonic acid (MOPS), 1 mM EDTA, and 10 mM dipicolinic acid (DPA), pH 7.5, followed by dialysis against 25 mM MOPS, and 1 μM EDTA, pH 8.0. The enzyme was then concentrated using an Amicon Ultra Microcon centrifugal filtration device (10,000 MWCO) and the buffer was exchanged using a PD-10 gel filtration column (GE Healthcare) equilibrated with 25 mM MOPS, pH 8.0 (pretreated with metal chelating resin, Chelex 100). The metal content of the protein was determined by inductively coupled plasma emission mass spectroscopy (ICP-MS) (Department of Geological Sciences, University of Michigan). The final concentration of KDAC8 was determined by both OD_{280} (ε_{280} =52120 $M^{-1}cm^{-1}$, under denaturing conditions) and the absorbance change after reaction with 5,5'-dithiobis(2-nitrobenzoic acid) (ε_{412} =13,600 $M^{-1}cm^{-1}$).

Activity Assays

The catalytic activity of wild-type and mutant KDAC8 was measured using a commercially-available fluorescent assay (BIOMOL) with the Fluor de Lys KDAC8 substrate (Scheme 3.1). All assay buffers were pre-treated with Chelex resin (Bio-Rad) to remove trace divalent metal ions. Metal-free KDAC8 was reconstituted with Co^{2+} by incubation with a stoichiometric concentration of metal in assay buffer (25 mM Tris pH

8.0, 137 mM NaCl and 2.7 mM KCl). Stoichiometric trichostatin A (TSA), a potent inhibitor, was used to quench the reaction. Fluorescence was monitored at λ_{ex} = 340 and λ_{em} = 450 for the deacetylated and cleaved product, and at λ_{ex} = 340 and λ_{em} = 380 for the acetylated substrate. The amount of product formed was determined from a standard curve made up of known concentrations of products and substrates. The steady-state kinetic parameter k_{cat}/K_m was determined from initial reaction rates using 0.4 – 12 μM Co^{2+}-KDAC8 and 50 μM substrate in assay buffer at 25 °C. The IC_{50} for acetate was determined by measuring initial rates under these conditions in the presence of varying concentrations of acetate (0-200 mM). Since the substrate concentration in these assays is significantly below the value of K_m, the IC_{50} value should be equal to the K_I for acetate. The values for k_{cat}/K_m, and the inhibition free energies were calculated using:

Equation 1 :$(k_{cat}/K_m)_{obs} = k_{cat}/K_m / (1 + [I]/ IC_{50})$

Equation 2 : $\Delta\Delta G = -RT \ln [(IC_{50})^{R37A}/(IC_{50})^{WT}$

Equation 3: $\Delta\Delta G^{\ddagger} = -RT \ln [(k_{cat}/K_M)^{WT}/(k_{cat}/K_M)^{R37A}$

Secondary Structure determination of WT and mutant KDAC8

Circular dichroism experiments were conducted on an Aviv CD Spectrometer model 62DS (Aviv, Lakewood, NJ) using a 1 mm quartz cuvette. Zinc-bound wild-type and mutants KDAC8 were diluted into 10 mM MOPS pH 7.5 to a final concentration of 0.05 mg/mL. Spectra were an average of three scans recorded at 25˚C between 200 and 240 nm, and the spectrum buffer (10 mM MOPS, 1μM $ZnCl_2$) was subtracted. The molar ellipticity(θ) was calculated using the formula:

Equation 3: θ = (millidegrees / (pathlength in millimeters x molar concentration of protein x the number of residues)).

KDAC8	k_{cat}/K_m **($M^{-1}s^{-1}$)**	$IC_{50,\ Acetate}$ **(mM)**
Co(II)-WT	7400 ± 100	2.5 ± 0.3
Co(II)-R37A	14 ± 1	400 ± 60
Co(II)-R37E	0.19 ± 0.04	nd[b]

Table 4.1. Catalytic activity and acetate inhibition constant of wild-type and mutant HDAC8. Measured in 25 mM Tris pH 8.0, 137 mM NaCl and 2.7 mM KCl. [b]Not determined

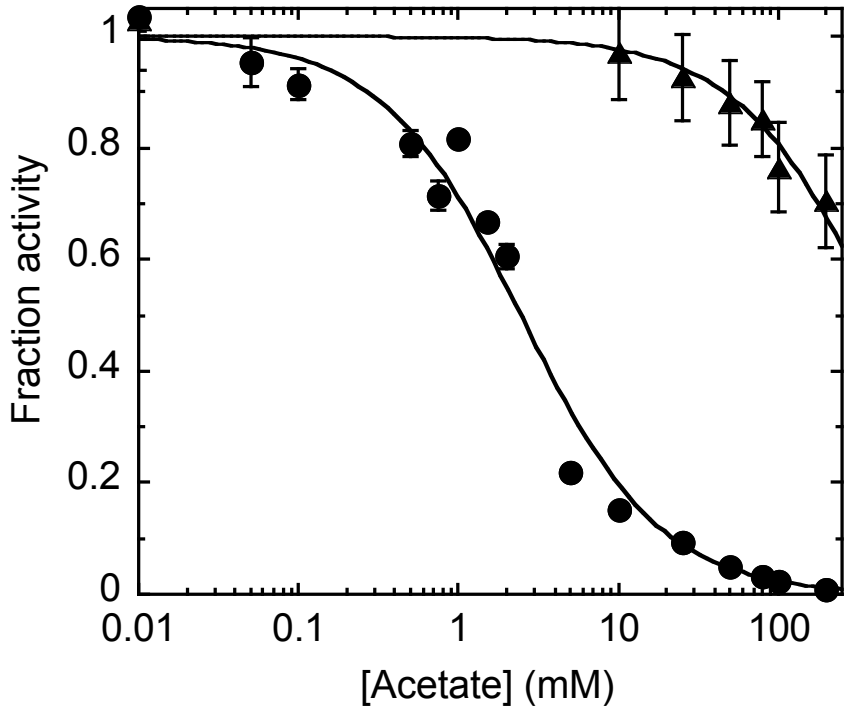

Figure 4.2. Inhibition of wild-type and R37A KDAC8 by acetate. 0.4 μM wild-type (circle) and 10 μM R37A (triangle) Co(II)-KDAC8 were incubated with varying concentrations of sodium acetate (0 – 200 mM) in 25 mM Tris pH 8.0, 137 mM NaCl and 2.7 mM KCl for 5 min before initiating the reaction by addition of 50 μM substrate (R-H-K(Ac)-K(Ac)-fluorophore) (BIOMOL). Initial rates were determined from a change in fluorescence. The fractional activity is the ratio of the initial rate in the presence ($(k_{cat}/K_m)_{Ac}$) and absence of acetate ($(k_{cat}/K_m)_0$) (note that the activity of R37A KDAC8 is decreased >500-fold compared to WT KDAC8). The value of IC_{50} is calculated from fitting $(k_{cat}/K_m)_{Ac}/(k_{cat}/K_m)_0 = 1 / (1 + [I]/ IC_{50})$ to the data.

Results

Reactivity of KDAC8_R37A

To experimentally examine the function of Arg37 in KDAC8, this residue was substituted with either alanine (R37A) or glutamate (R37E). Both of these mutant enzymes were expressed as recombinant proteins in *E. coli* to levels similar to that of wild-type (WT) KDAC8 and purified as described for WT KDAC8. The catalytic activity of these two mutants is decreased enormously compared to WT KDAC8, as measured from the deacetylation of the Fluor de Lys KDAC8 substrate (R-H-K(Ac)-K(Ac)-fluorophore) catalyzed by the Co^{2+}-substituted enzymes. The values for k_{cat}/K_M decrease by 528-fold for removal of the side chain (R37A) and by 4 x 10^5-fold for substitution of arginine with the negatively charged glutamate (Table 1). These data demonstrate that the positively charged side chain at position 37 is important for the high catalytic activity of KDAC8, even though it is located 9 Å from the catalytic zinc ion.

Acetate affinity for KDAC8

To examine whether Arg37 affects the affinity of KDAC8 for acetate, we measured the IC_{50} value for inhibition of turnover by acetate for recombinant wild-type and R37A HDAC8. For WT KDAC8, the initial rate for deacetylation is decreased by the addition of the product, acetate, with an IC_{50} value of 2.5 mM. These concentrations of sodium acetate have little to no affect on the ionic strength of the assay. However, for the R37A mutant, the initial rate of deacetylation is unaffected by the addition of small

concentrations of acetate; the measured value for the IC_{50} is increased 160-fold to 400 ± 60 mM, assuming complete inhibition at saturating acetate (Figure. 4.2). This number is a lower limit for the value of IC_{50} as the increased concentration of sodium in the assay may also inhibit turnover. The IC_{50} values are directly comparable and approximate the inhibition constant, K_i, assuming that acetate is competitive with substrate, since the substrate concentration in the activity assays is significantly below the substrate K_M for both enzymes. Therefore, the affinity of WT KDAC8 for acetate is at least 3 kcal/mol greater than that of the R37A mutant. Furthermore, the transition state stabilization for deacetylation ($\Delta\Delta G^{\ddagger}$) determined from the k_{cat}/K_m, conferred by the R37 side chain is only slightly higher in energy (3.5 kcal/mol) than the enhancement of the acetate affinity.

Secondary structure effects of R37A

To investigate the impact of mutations at R37 on the secondary structure of KDAC8, we measured the circular dichroism (CD) spectrum. For WT-KDAC8, the CD spectrum has a minimum at 222 nm with a shape that is characteristic of α-helical structure, consistent with previously published results. The CD spectrum of the R37A KDAC8 mutant is nearly identical to that of WT, indicating that the overall structure is unaffected by deletion of the R37 side chain. In contrast, the molar ellipticity at most wavelengths is significantly decreased in the CD spectrum of R37E (figure. 4.3). These results suggest that the decrease in k_{cat}/K_M observed in R37A KDAC8 is primarily due to a perturbation in the catalytic mechanism rather than a change in the structure of the enzyme while the additional decrease in k_{cat}/K_M observed for the R37E mutant is at least partially due to global unfolding of this protein.

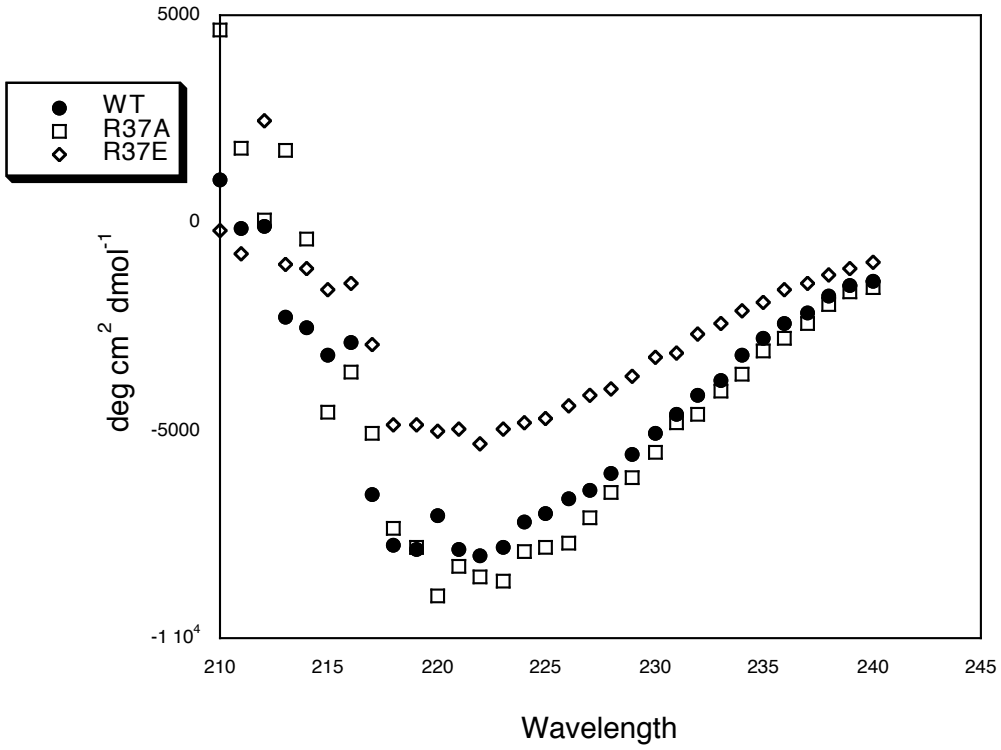

Figure 4.3. CD spectra of wild-type, R37A, and R37E KDAC8. All enzymes were reconstituted with stoichiometric zinc and then diluted to a final concentration of 1 μM in 10 mM MOPS pH 7.5. Each spectrum of HDAC8 (wild-type (closed circle), R37A (open square) and R37E (open diamond)) is an average of three scans with the spectrum of the buffer subtracted. The molar ellipticity (θ) was calculated using the formula: θ = (millidegrees / (pathlength in millimeters x molar concentration of protein x the number of residues)).

Computational analysis of Arg37 in the internal cavity

To test the hypothesis that the Arg37 mediates the shuttling of acetate and water through the 14 Å channel we collaborated with Dr. Matthew Fuchner at the Imperial College, London to carry out molecular dynamics simulations. The crystal structure visualized the tunnel in a closed state Arg37 interactions form a barrier between the active site and the external surface of the protein. Molecular dynamics (MD) simulation designed to examine the dynamics of the channel in a closed state demonstrated that the diameter of the passage remained in the closed state (2.89 Å) over the course of the 20 ns simulation. Furthermore, the interactions between Arg37 and Gly303 and Gly305 are also maintained throughout the course of the simulations. Analysis of the water trajectories within the KDAC8 channel reveal that solvent water molecules are positioned within 2.5 Å on either side, but cannot cross, the barrier maintained by the G139-G303 interactions (at least on a 20 ns timescale). These distances are consistent with the closed state of the channel and persist throughout the simulation time. Next, our collaborators computationally mutated Arg37 to Ala (R37A) and carried out a MD simulation. This change in structure did not alter the dynamics of channel opening within the timescale of the simulation. These results suggest that significant structural reorganization, including rearrangement of the Arg37 side chain to disrupt the interactions with Gly303 and Gly305 and, in turn, to break interactions with Gly139, would be required to open the 14 Å channel. Furthermore, these data indicate that the structure of the open conformation

would be quite different from the existing stable closed state, which the MD simulation is unable to reproduce on a 20 ns timescale.

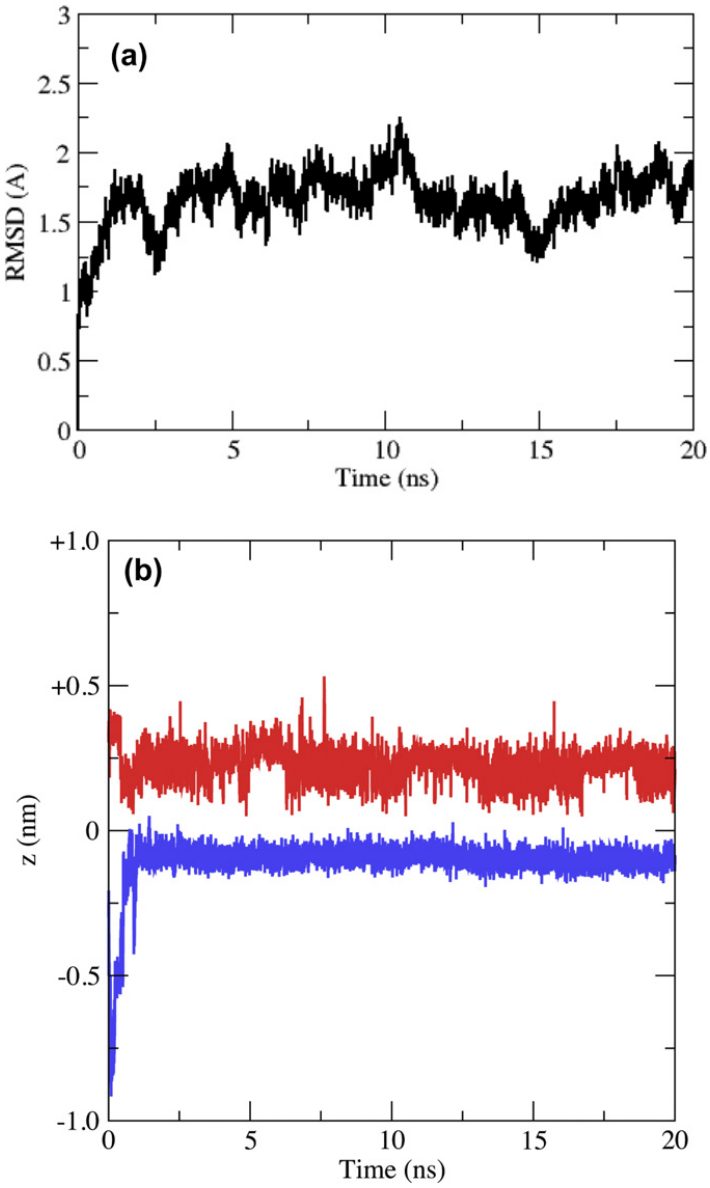

Figure 4.4[3] . MD simulation of Arg 37 in KDAC8 a) Plot of the Ca root mean squared deviation (RMSD) from the initialcrystal structure of KDAC8, plotted as a function of time. The average RMSDmeasured over the course of 20 ns simulation is 1.65 Å. b) Trajectories of two watermolecules that come very close to the G139–G303 interaction

[3] Figure 4.4 was made and analyzed by Matthew Fuchtner.

but are unable to cross it. Figure (a) and (b) do not use the same distance scale.

Discussion

These data demonstrate that the R37 side chain is crucial for enhancement of both the catalytic activity and acetate affinity of KDAC8. In the R37A mutation, a short hydrophobic side chain of Ala replaces the longer, charged side chain of Arg that significantly decreases catalytic activity and acetate affinity while maintaining proper secondary structure. The computational simulation failed to demonstrate opening and closing of the internal channel, where the Gly139-Gly303 interaction anchored by Arg37 behaves like a gate for the internal channel. This sheds doubt on the proposed function of this channel for regulating transit of water or acetate form the active site. Furthermore, since the catalytic effects of the Arg37A are on the k_{cat}/K_m, the decreased activity of the R37A mutant is not due to slow acetate dissociation. Since the Arg37 side chain is located 12 Å away for the catalytic zinc and 14 Å from the carbonyl oxygen of the substrate, this side chain also does not stabilize the transition state by direct contact, unless a large conformational change occurs. Therefore, the Arg37 side chain likely affects catalysis indirectly either via long-range electrostatic or structural effects. Nonetheless, this alteration does have a large effect on activity suggesting that compounds bound to the channel could also be inhibitors.

In summary, we have performed both experimental and computational studies revealing that Arg37 is a crucial residue within the internal cavity of KDAC8.

Experimentally, Arg37 provides significant stabilization of both bound acetate and the catalytic transition state, as indicated by the loss of activity in the R37A mutation.

BIBLIOGRAPHY

1. Finnin, M. S., Donigian, J. R., Cohen, A., Richon, V. M., Rifkind, R. A., Marks, P. A., Breslow, R., and Pavletich, N. P. (1999) *Nature* **401**, 188-193

2. Vannini, A., Volpari, C., Filocamo, G., Casavola, E. C., Brunetti, M., Renzoni, D., Chakravarty, P., Paolini, C., De Francesco, R., Gallinari, P., Steinkühler, C., and Di Marco, S. (2004) *Proceedings of the National Academy of Sciences of the United States of America* **101**, 15064-15069

3. Witt, O., Deubzer, H. E., Milde, T., and Oehme, I. (2009) *Cancer letters* **277**, 8-21

4. Marks, P. A. (2010) *Biochim Biophys Acta* **1799**, 717-725

5. Karagiannis, T. C., and El-Osta, A. (2007) *Leukemia* **21**, 61-65

6. Richon, V. M., Emiliani, S., Verdin, E., Webb, Y., Breslow, R., Rifkind, R. A., and Marks, P. A. (1998) *Proceedings of the National Academy of Sciences of the United States of America* **95**, 3003-3007

7. Furumai, R., Matsuyama, A., Kobashi, N., Lee, K. H., Nishiyama, M., Nakajima, H., Tanaka, A., Komatsu, Y., Nishino, N., Yoshida, M., and Horinouchi, S. (2002) *Cancer Res* **62**, 4916-4921

8. Haberland, M., Montgomery, R. L., and Olson, E. N. (2009) *Nat Rev Genet* **10**, 32-42

9. Balasubramanian, S., Verner, E., and Buggy, J. J. (2009) *Cancer letters* **280**, 211-221

10. Fulda, S., and Debatin, K.-M. (2005) *Cancer biology & therapy* **4**, 1113-1115

11. Rundlett, S. E., Carmen, A. A., Kobayashi, R., Bavykin, S., Turner, B. M., and Grunstein, M. (1996) *Proceedings of the National Academy of Sciences of the United States of America* **93**, 14503-14508

12. Wang, D.-F., Wiest, O., Helquist, P., Lan-Hargest, H.-Y., and Wiech, N. L. (2004) *Journal of medicinal chemistry* **47**, 3409-3417

13. Wang, D.-F., Helquist, P., Wiech, N. L., and Wiest, O. (2005) *Journal of medicinal chemistry* **48**, 6936-6947

CHAPTER V

CONCLUSIONS AND FUTURE DIRECTIONS

Conclusions

Lysine acetylation is a key post-translational modification of many proteins in mammalian cells. Dynamic control of acetylation by lysine acetyl transferases (KATs) and lysine deacetylases (KDACs) regulates the function of many proteins that operate in numerous cellular processes. Furthermore, inhibitors targeting KDACs are effective in activating the transcription of genes responsible for tumor cell growth suppression and apoptosis. Inhibition and knockout studies have also demonstrated important roles of KDACs in signaling, gene regulation, and protein folding. Particularly, KDACs act on substrates to regulate their stability, function, and interaction with other proteins (1-3). Therefore, normal cells maintain strict control of KDAC activity to ensure proper cellular function.

Eukaryotic genome encodes 18 forms of KDACs while over 3000 acetylated proteins are found in the cell. Hence, these 18 KDACs must catalyze deacetylation of multiple substrates but each isozyme likely has specific substrates. Class I KDACs (1-3, 8) are ubiquitously expressed. Class II KDACs have distinct roles in development as they

are highly enriched in the brain, muscle, heart, and thymus. Genetic deletion of these KDACs generally results in embryonic lethality. These KDACs are able to shuttle between the nucleus and cytoplasm suggesting they also have redundant roles in the cell. Hence, KDACs act on substrates in the cytoplasm and nucleus of many tissues and could have a role in virtually all cellular processes(4).

Many studies have examined the effects of post-translational modifications such as phosphorylation on the regulation of KDAC activity(5). These studies show that phosphorylation of KDAC generally, modulates their localization. Second, several reports have shown that the modification of KDAC substrates competes with KDAC activity, such as histone substrates that can be either methylated or acetylated(6,7). Last, KDAC association with large protein complexes also regulates their activity. This work focuses on the role that the bound metal-ion plays in the activity and substrate specificity of KDACs.

The metal ion is necessary for deacetylase activity. Trapoxin, the first known KDAC inhibitor, features a metal binding domain. Trapoxin-mediated isolation of KDAC gave the first clue about the importance of the divalent metal ion for these enzymes. To date, the most potent and specific KDAC inhibitors possess a metal binding domain underlining the importance of the divalent metal ion in the activity of KDACs. Consistent with most mononuclear metalloenzymes, it was expected that the KDAC mechanism would mirror all of the general features of metal-catalyzed hydrolytic enzymes. Namely, the metal ion activates the enzyme activity by polarizing of the substrate and activating the water nucleophile, and stabilizing charge in the tetrahedral intermediate and the transition state. Thus, it was intriguing when it was reported that KDAC8 exerts differing

catalytic efficiency with bound Fe^{2+}, Co^{2+} or Zn^{2+}(8). Close structural analysis of KDAC8 reveals that the substrate-binding site is lined by (8) loops indicating that this enzyme has some flexibility in substrate recognition(9). Accordingly, we hypothesized that the catalytic metal ion could induce a specific conformation that alters the substrate specificity of KDAC.

We focused our study on elucidating the metal-dependent regulation of KDAC. First, we probed the role that the divalent metal ion plays in the substrate recognition of KDAC8 by examining the reactivity of Zn^{2+} and Fe^{2+}-bound KDAC8 on a library of peptide substrates (GXK(Ac)ZGC) using matrix-assisted laser desorption ionization time-of-flight mass spectrometry (MALDI TOF MS) spectra of the immobilized peptide substrate before and after treatment with metal-bound KDAC8. The reactivity of Zn^{2+} and Fe^{2+}-KDAC8 with this peptide library resulted in sets of substrates that were specific for Zn^{2+}-KDAC8, Fe^{2+}-KDAC8 or similar reactivity for both. Steady-state kinetic analysis of KDAC8 catalyzed deacetylation of the peptide substrates selected from each substrate profile confirms that these peptides retain their characteristics. Together these results demonstrate that the substrate specificity of KDAC8 is regulated by divalent metal ion bound to the active site.

Second, we purify KDAC11 from *E. coli* and tested its substrate selectivity. We showed that KDAC11 activity is also modulated by metal ions. Due to the low activity on the coumarin substrate, we screened the reactivity of KDAC11 with a library of 384 peptides (GXK(Ac)ZGC) to identify a suitable substrate for biochemical characterization of KDAC11. Unlike KDAC8, KDAC11 shows specific sequence preferences. The highest deacetylase activities were observed for Co^{2+}–bound KDAC11 in three peptides

(GFK(Ac)LGC, GPK(Ac)LGC, GYK(Ac)LGC). Excitingly, the sequence GPK(Ac)LGC bears a close resemblance to Cdt1, a DNA replication licensing factor and proposed KDAC11 substrate. We measured the steady-state kinetic parameter for the IIAPPKLAC peptide. The k_{cat}/K_m for deacetylation of this sequence catalyzed by Zn^{2+}-bound KDAC11 is 1333-fold larger than the commercially available coumarin substrate, validating the superiority of this peptide as a KDAC11 substrate. Furthermore, the reactivity of KDAC11 with this sequence varies with the active site divalent metal ions (Fe^{2+}>Zn^{2+}), a property also observed in KDAC8.

Last, we evaluated the function Arg37 in KDAC8, implicated by the crystal structure of KDAC8, in catalysis. Substitution of Arg37 with either alanine (R37A) or glutamate (R37E) results in a 528-fold decrease in k_{cat}/K_M for the alanine mutant and 4 x 10^5-fold for R37E mutant. Secondary structure analysis revealed that the Arg37A secondary structure is nearly identical to that of WT, indicating that the overall structure is unaffected by deletion of the Arg37 side chain. Furthermore Arg37 affects the interaction of KDAC8 with acetate, as the measured IC_{50} value for inhibition of turnover by acetate is increased by 160-fold in the R37A mutant. Altogether, these results show that Arg37 is important for catalysis and acetate affinity, and this can be potentially exploited for specific inhibition of KDAC.

Future Directions

This study provides compelling evidence for the critical role of metal ions in the regulation of KDACs. Future studies will evaluate the metal-dependent substrate specificity *in vivo*. KDACs represent an ideal platform to probe the metal ion regulation

of substrate specificity in mammalian cells. Pull-down studies using a bacterial deacetylase (LpxC) demonstrate switching of metal ions in response to nutritional changes. In the presence of high zinc in the media, the metal bound to LpxC switches from Fe^{2+} to Zn^{2}. However, LpxC recognizes only one substrate. KDACs recognize many substrates. Isolation of KDACs from mammalian cells and analysis of the bound metal ion will greatly aid in understanding the *in vivo* regulation of KDACs by divalent metal ions.

Furthermore, several KDACs operate in protein complexes that function in diverse cellular processes. In addition to altering substrate specificity, it is possible that the divalent metal ion regulates the interaction of KDACs with proteins complexes. By identifying binding partners, one could investigate these interactions and possibly pinpoint areas in the proteins that the metal ion shapes and facilitates binding. These data would aid in the development of specific inhibitors that target these binding interactions.

The peptide library studies are the first study that analyzed the role of the metal ion in the regulation of KDAC substrate specificity. We are currently collaborating computational chemists to develop algorithms to predict substrates of $Fe^{2+}$and Zn^{2+}-bound KDAC8. The peptide library analyses KDAC8 under a specific set of conditions. However, cellular conditions are dynamic meaning that they change in response to internal and external stimuli. Since, these results show that KDAC8 has metal ion dependent specific substrates, it is possible that alteration in the intracellular metal concentrations, perhaps due to redox stress, could alter the activity and substrate selectivity of the KDACs.

KDAC11 is a unique deacetylase since it belongs to a class by it-self. The substrate selectivity of KDAC11 shows that it has a unique sequence preference. The sequence motif identified from the peptide library studies is validated as a recognition site for this enzyme *in vivo* by the similarity of the Cdt1 sequence. Therefore, an analysis of the acetylated protein library could provide a list of potential proteins substrates for KDAC11. KDAC11 was successfully characterized primarily because we controlled the metal stoichiometry and monovalent cation concentrations. Most attempts at recombinant expression purification of KDACs from *E. coli* have been difficult. Consequently, successful isolation and biochemical characterization of each KDAC isozyme will involve a detail investigation of divalent and monovalent cation dependence as well as the substrate preferences.

Finally, screens for inhibitors of metal-dependent KDACs are usually done either with purified, commercially available KDACs or in cell lysates aerobically. Therefore, the active site metal ion is Zn^{2+} and additional Zn^{2+} in the assays could lead to inhibition of KDAC. These confounding issues with the active site metal ion could lead to incorrect identification of the best inhibitors from initial screens. Preferentially, these inhibitor screens should be performed with purified KDAC with a stoichiometric metal ion, preferably the metal used *in vivo.* Our data show that KDAC8 is generally most active when bound to Fe^{2+} (Figure 2.2) and *in vivo* data indicate that KDAC8 activity is oxygen-sensitive (S. Gattis, personal communication) suggesting the formation of Fe^{2+}-KDAC8 *in vivo*. However, due to the reactivity with oxygen, measurement of the activity of Fe^{2+}-KDAC8 must be done anaerobically. Therefore, an inhibitor screen with Fe^{2+}-bound KDAC8 would be prohibitively difficult. A possible reasonable mimic of Fe^{2+}-KDAC is

the Co^{2+}-bound form. Reactions of Co^{2+}- and Fe^{2+}-KDAC8 with a peptide library (see comparison in Figure 5.1) show that Co^{2+}-KDAC8 generally catalyzes the deacetylation of acetylated peptides more rapidly than either the Fe^{2+}- or Zn^{2+}-bound enzymes. However, the substrate selectivity of Co^{2+}-KDAC8 is more similar to the Fe^{2+}-enzyme as a number of the Fe^{2+}-specific peptides are readily deacetylated by Co^{2+}-KDAC8. Therefore, the cobalt-bound KDAC8 better mimics the activity of the Fe^{2+}-enzyme and is recommended for use in the screens for KDACi.

Closing remarks

In brief, KDACs play a fundamental role in many cellular processes. In normal cells, proper regulation of KDAC activity is necessary. Sustained activity of KDACs in tumor cells leads to proliferation, invasion. Since the bound catalytic metal is central to their activity and molecular recognition, a detailed understanding of role of the metal ion in the structure and function of KDACs will aid in understanding the specific role of these enzymes in eukaryotic cells and will be crucial to exploitation of this protein family for therapeutic inhibition in a variety of diseases.

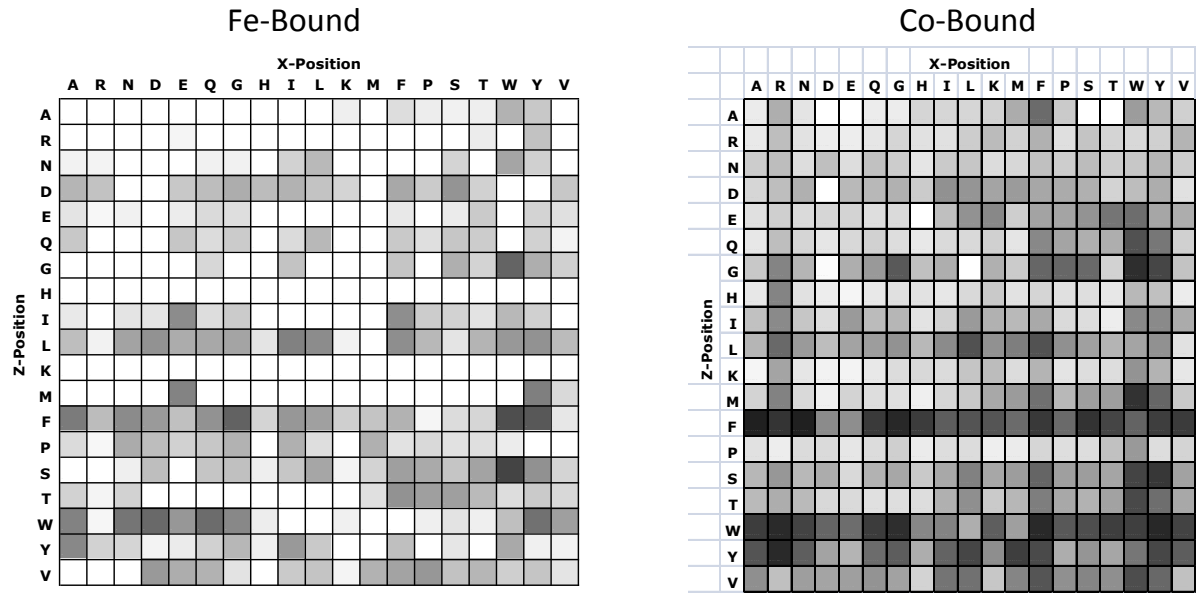

Figure 5.1 Substrate selectivity of Fe^{2+} and Co^{2+}-bound KDAC8. GXK(Ac)ZGC peptide library (X and Z represent all AAs except Cys). The assays were done using MALDITOF (Figure2.1). The substrate plates were incubated with 1 µM Fe^{2+}- or Co^{2+}-KDAC8 in 25 mM Tris pH 8, 137 mM NaCl, 2.7 mM KCl, 30°C for 1 h.

BIBLIOGRAPHY

1. Haberland, M., Montgomery, R. L., and Olson, E. N. (2009) *Nat Rev Genet* 10, 32-42

2. Johnstone, R. W. (2002) *Nature reviews. Drug discovery* 1, 287-299

3. Witt, O., Deubzer, H. E., Milde, T., and Oehme, I. (2009) *Cancer letters* 277, 8-21

4. Wu, X., Oh, M.-H., Schwarz, E. M., Larue, C. T., Sivaguru, M., Imai, B. S., Yau, P. M., Ort, D. R., and Huber, S. C. (2011) *Plant Physiology* 155, 1769-1778

5. Sengupta, N., and Seto, E. (2004) *Journal of cellular biochemistry* 93, 57-67

6. Gurard-Levin, Z. A., and Mrksich, M. (2008) *Biochemistry* 47, 6242-6250

7. Heltweg, B., Dequiedt, F., Marshall, B. L., Brauch, C., Yoshida, M., Nishino, N., Verdin, E., and Jung, M. (2004) *Journal of medicinal chemistry* 47, 5235-5243

8. Gantt, S. L. (2006) Human Histone Deacetylase 8: Metal Dependence and Catalytic Mechanism. in *Biologican Chemistry*, University of Michigan, Ann Arbor, MI

9. Vannini, A., Volpari, C., Filocamo, G., Casavola, E. C., Brunetti, M., Renzoni, D., Chakravarty, P., Paolini, C., De Francesco, R., Gallinari, P., Steinkühler, C., and Di Marco, S. (2004) *Proceedings of the National Academy of Sciences of the United States of America* 101, 15064-15069